Accepted Manuscript

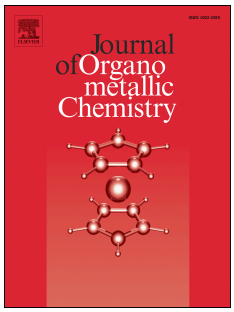

Microsolvation, aggregation, and pseudomonomolecular, ionic sp^2-stereoinversion mechanism of two exocyclic β,β-di-*tert*-alkyl-α-arylvinyllithiums

Rudolf Knorr , Karsten-Olaf Hennig , Petra Böhrer , Bernhard Schubert

PII: S0022-328X(14)00277-0

DOI: 10.1016/j.jorganchem.2014.05.031

Reference: JOM 18603

To appear in: *Journal of Organometallic Chemistry*

Received Date: 29 March 2014

Revised Date: 21 May 2014

Accepted Date: 27 May 2014

Please cite this article as: R. Knorr, K.-O. Hennig, P. Böhrer, B. Schubert, Microsolvation, aggregation, and pseudomonomolecular, ionic sp^2-stereoinversion mechanism of two exocyclic β,β-di-*tert*-alkyl-α-arylvinyllithiums, *Journal of Organometallic Chemistry* (2014), doi: 10.1016/j.jorganchem.2014.05.031.

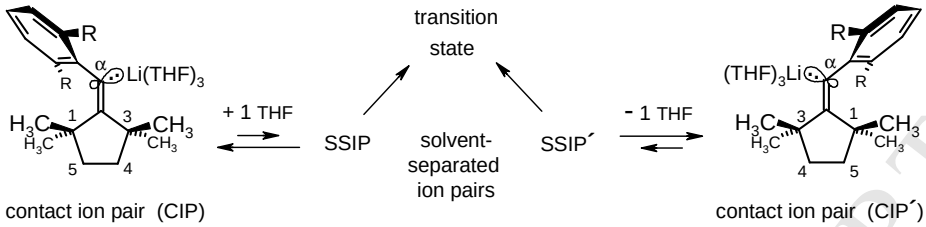

The pseudomonomolecular (THF-catalyzed) rate constants k_ψ of cis/trans interconversion of the trisolvated, monomeric ground-states CIP and CIP´ in THF via solvent–separated ion pairs (SSIP) can be measured through line shape analyses of the pairwise "coalescing" (averaging) NMR signals of diastereotopic ^{1}H and ^{13}C nuclei at positions 1/3 and 4/5.

Microsolvation, aggregation, and pseudomonomolecular, ionic sp^2-stereoinversion mechanism of two exocyclic β,β-di-*tert*-alkyl-α-arylvinyllithiums[§]

Rudolf Knorr*, Karsten-Olaf Hennig, Petra Böhrer, Bernhard Schubert

Address: Department Chemie, Ludwig-Maximilians-Universität München, Butenandtstrasse 5-13 (Haus F), 81377 München, Germany

Email: Rudolf Knorr* - rhk@cup.uni-muenchen.de

* Corresponding author

Abstract

A THF-solvated, crystalline, exocyclic alkenyllithium, (*tert*-alkyl)$_2$C=C(Li)–Ph, was synthesized and shown to be a disolvated dimer in the solid state and in toluene as the solvent; increasing amounts of the monomeric species emerged on cooling the toluene solution. In THF as the solvent, only the trisolvated monomer was present and identified as a contact ion pair (CIP) through its scalar $^{13}C,^{6}Li$ NMR coupling. This ground-state needs only one further THF ligand as a catalyst for breaking the C–Li bond with formation of a tetrasolvated, solvent-separated ion pair (SSIP) on the way to the transition state of cis/trans sp^2-stereoinversion. The ensuing pseudomonomolecular, ionic mechanism is confirmed by low pseudoactivation parameters: enthalpy $\Delta H_\psi^\ddagger$ = 6.9(3) kcal mol^{-1}; entropy $\Delta S_\psi^\ddagger$ = –23.3(9) cal mol^{-1} K^{-1}. Similar parameters were found with 2,6-dimethylphenyl in place of Ph.

This article is dedicated to Professor Paul Knochel in recognition of his kind support.

Keywords.

Monomeric alkenyllithiums; $^{13}C,^{6}Li$ NMR coupling; ionization mechanism; pseudoactivation parameters; sp^2-stereoinversion; THF catalysis

1. Introduction

The characterization of organolithium compounds in solution is incomplete without knowledge of the microsolvation numbers *d*, which state how many electron-donor ligands (other than the carbanionic centers) are coordinated to a lithium cation. For example, the monomeric α-phenyl-α-lithioalkene **1a** is trisolvated (*d* = 3) in tetrahydrofuran (THF) as the solvent but disolvated (*d* = 2) in Et_2O or in *tert*-butyl methyl ether (*t*BuOMe) [1]. The neglect of such microsolvation or the use of incorrect *d* data can lead to wrong entropy values, as exemplified for the dimerization equilibria [2] of **1a** and **1c** in toluene as the solvent. Unfortunately, microsolvation numbers at Li are most often not accessible for monodentate (nonchelating) ethereal ligands (Et_2O, THF, etc.), because NMR spectroscopy usually cannot directly distinguish the ligand fraction coordinated at Li from the noncoordinated ("free") portion if ligand interchange between these two situations is very fast on the NMR timescale, so that only averaged ligand signals can be detected. Sufficiently slow ligand scrambling was observed for C–Li compounds with the very strong donor ligand $(Me_2N)_3PO$ (HMPA) [3], with THF at the endocyclic Li of dimeric $Me_2CuLi\&LiCN$ [4], with intramolecular (chelating) donor functions [5], and with *t*BuOMe, Et_2O, or THF at our sterically congested model system **1** [1].

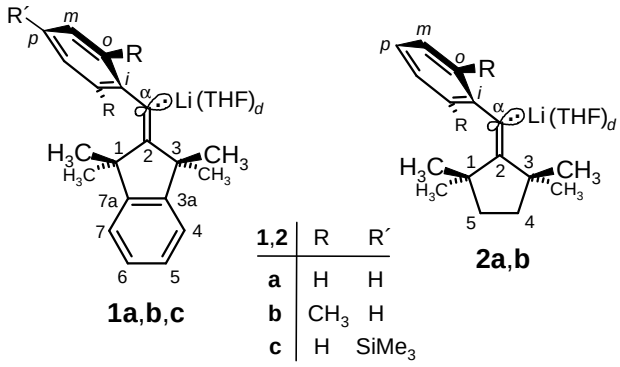

Scheme 1. The α-arylalkenyllithiums **1** and **2**.

This inability of measuring microsolvation numbers d directly may be circumvented by means of an empirical [1] relationship (eq 1) of d with the scalar, one-bond spin-spin coupling constant $^{1}J_{C,Li}$ between a carbanionic ^{13}C nucleus and a ^{6}Li atom; the ^{6}Li isotope is known [6] to be generally preferable to the more abundant isotope ^{7}Li in ^{13}C NMR measurements. In eq 1, n is the number of Li cations in direct contact with the inspected (^{13}C NMR) carbanionic center and a is the number of carbanionic centers bound directly to a Li cation, so that $n = a = 1$ for monomers, $n = a = 3$ for cubane-like tetramers [7], and $n = a = 2$ for dimers or for "static" (nonfluxional) [1] cyclooligomers. The sensitivity factors L in eq 1 apply to both the monomers and the aggregates within a family of C–Li compounds [8]: L = 63 (± 3) Hz for *n*-alkyllithiums (but 68.4 Hz for Me_4Li_4), 60 (± 2) for neopentyllithium, 56 (± 1) for *s*-alkyllithiums, 47.5 (± 1) for *tert*-butyllithium (*t*BuLi), 42 (± 2) for 1-aryl-1-alkenyllithiums [but 69 (± 2) for dimeric and tetrameric H_2C=CH–Li], 62 (± 3) for phenyllithium, and 69 (± 3) Hz for alkynyllithiums.

$$^{1}J_{C,Li} = L \times [n \times (a + d)]^{-1} \qquad (1)$$

Generally, scalar coupling between the nuclear spins in ^{13}C–^{6}Li bonds can only be observed under conditions of a sufficiently slow *inter*molecular scrambling of the Li cations (usually at low temperatures). Due to the spin quantum number $I = 1$ of the ^{6}Li nucleus, the coupling with one ($n = 1$) ^{6}Li will split a ^{13}C NMR signal into $2nI+1 = 2n+1 = 3$ components with a

1:1:1 intensity pattern; such a triplet provides evidence for a monomeric state unless the molecule bears a Lewis-basic heteroatom X that can coordinate to the Li cation of a second molecule, thus forming aggregates which carry C–Li–X units. The contact of a ^{13}C center with two ^{6}Li nuclei (n = 2) will become evident through a 1:2:3:2:1 quintet splitting which establishes the CLi_2 units of a dimer and also those of a "static" cyclooligomer, namely, without *intra*aggregational ("fluxional") scrambling [9] of more than two Li cations. With these reservations, the ^{13}C NMR splitting multiplicity can identify n and hence the aggregational state (since normally $a = n$ in eq 1); if so, the magnitude of $^{1}J_{C,Li}$ (to be read from the frequency intervals in the multiplets) can provide the microsolvation numbers d. The relationship of eq 1 was discovered [1] because steric shielding in **1a** and **1c** impeded the scrambling of coordinated with free monodentate donor ligands (THF, Et_2O, *t*BuOMe) to such an extent that d could be measured for the dimers and for some of the monomers of **1** at low temperatures by ^{1}H and/or ^{13}C NMR integration. On this footing and with the above-mentioned sensitivity factor of L = 42 (± 2) Hz in eq 1, the microsolvation numbers d of the α-aryl-β,β-di-*tert*-alkylvinyllithiums **2a** and **2b** studied in this work should be indicated by the following prospective $^{1}J_{C,Li}$ values: 10.5 (± 0.5) Hz for a trisolvated monomer (d = 3), 14.0 (± 0.7) Hz for a disolvated monomer (d = 2), 7.0 (± 0.4) Hz for disolvation of a CLi_2 structural motif (d = 1 per lithium), or 5.3 (± 0.3) Hz for a tetrasolvated CLi_2 motif (d = 2). The results should enable us to decide whether the recently [10] established pseudomonomolecular, ionic mechanism of sp^2-stereoinversion applies also to **2a** and **2b**.

2. Results and discussion

2.1. Synthesis and ground-state properties of alkenyllithium ***2a***

Pursuing a strategy described [11] for the precursors of **1a**, we heated the known [12] alcohol **3** (Scheme 2) for a short time with an excess of *N*-bromosuccinimide (NBS) to

produce the α-monobromide **4**, taking care to avoid overbromination that would form the corresponding α,α-dibromide whose rapidly ensuing ring expansion was shown to generate the bromoketone **7**. The analogous, slower ring expansion of monobromide **4** to give the halogene-free ketone **8** [13] is expecially threatening for solvent-free **4**, so that crude **4** should be dehydrated by $SOCl_2$ immediately to furnish the crystalline bromoalkene **5** which had previously [14] been obtained as a liquid on a different route. (A further alternative synthesis of **5** from the olefin **9a** is reported in the Supplementary Material.)

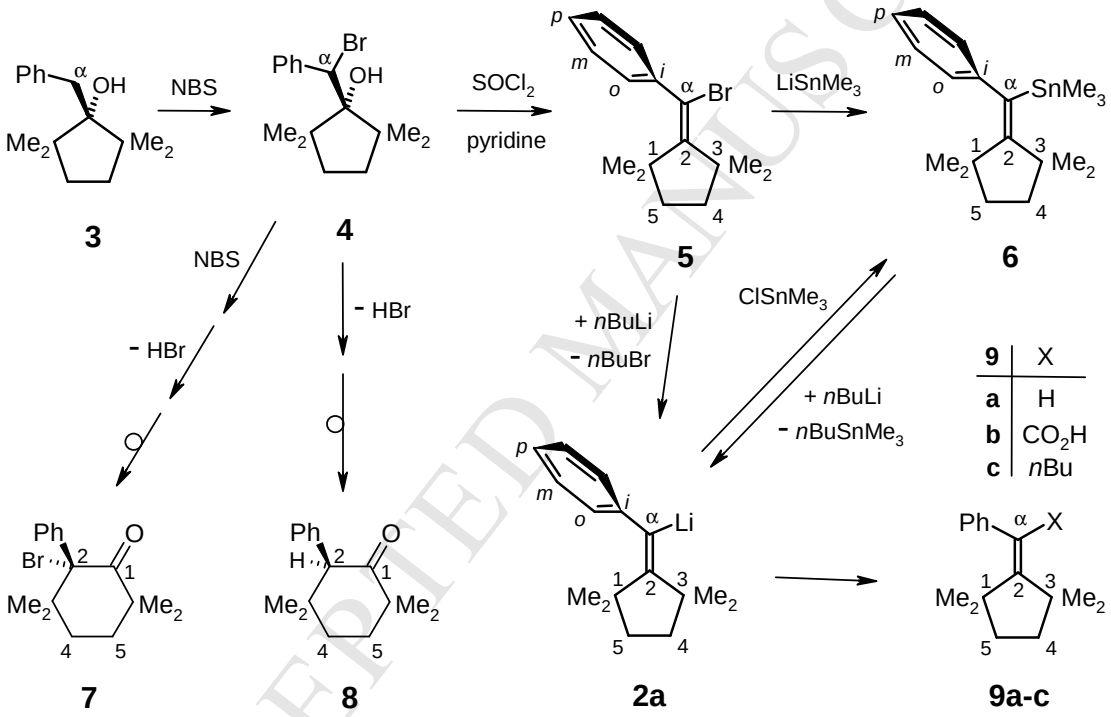

Scheme 2. Synthesis and derivatives of **2a**.

The Br/Li interchange reaction between bromoalkene **5** and *n*-butyllithium (*n*BuLi) generated the alkenyllithium **2a** (Scheme 2) along with 1-bromobutane (*n*BuBr); this interchange occurred in cyclopentane solution even in the absence of donor molecules at room temperature (r.t.), as witnessed after one week by quenching with solid CO_2 and isolation of the acid **9b**. Prepared from **5** more rapidly in *t*BuOMe or Et_2O as the solvents with ca. two equivalents of *n*BuLi, **2a** decayed slowly (in > 19 hours at r.t.) to furnish the "parent" olefin

9a, whereas **2a** in THF reacted quickly with the concomitant *n*BuBr to afford the α-butyl derivative **9c** (not detected in *t*BuOMe or Et_2O). Generated from **5** in *t*BuOMe with *n*BuLi, **2a** was also trapped after 20 min at 20 °C by Me_3SnCl to give the α-$SnMe_3$ derivative **6** (39%) and olefin **9a** (44%). In a slightly more productive alternative process, a mixture of **6** and **9a** (78:22) was obtained from bromoalkene **5** with $LiSnMe_3$ [15] in THF as the solvent. These two stannylation reactions opened a route to cleaner and more stable samples of **2a**: the subsequent treatment of pure **6** with *n*BuLi furnished **2a** along with *n*$BuSnMe_3$, *n*Bu_2SnMe_2, and methyllithium, thus avoiding the formation of disturbing coproducts (LiBr or *n*BuBr). After this practically instantaneous Sn/Li interchange reaction, **2a** in THF decayed through proton transfer from the solvent to give olefin **9a** and ethylene with a first half-life time of ca. 5.5 hours at 23 °C: quenching with D_2O after 6 hours afforded **9a** and [α-D]**9a** (58:42) exclusively. The Sn/Li interchange was slower in *t*BuOMe as the solvent; it did not occur in pentane alone (> 24 hours), but it proceeded slowly (overnight) in pentane after the addition of THF (three equiv) and produced of (**2a**&THF)$_2$ as single crystals which could be purified through washing with (cyclo)pentane and were well suited for NMR or X-ray analyses. An analogous run with Et_2O (three equiv) in place of THF required three days in pentane at 20 °C and produced crystals that were unsuitable because they dissolved quickly above –70 °C in pentane.

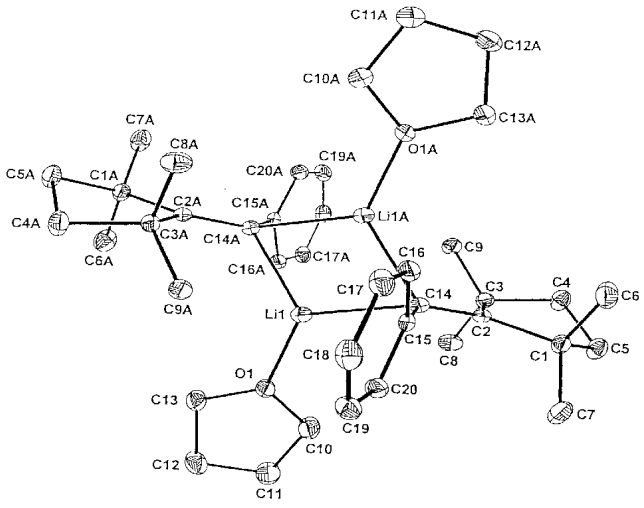

Figure 1. Solid-state structure of (**2a**&THF)$_2$ at –100 °C, with the crystallographic numbering and thermal ellipsoids of 25% probability.

The X-ray analysis revealed a centrosymmetric, disolvated dimer (**2a**&THF)$_2$ with one THF ligand (*d* = 1) at each Li atom. The planar four-membered ring Li$_2$(C14)$_2$ and the plane of the C2/C14 (C-2/C-α) double bond (Figure 1) enclose an interplanar angle of 104°. This angle and many of the other geometric parameters [13] resemble those of crystalline (**1a**&THF)$_2$ [1]; however, all crystalline dimers [1] of **1a** and **1c** had practically planar indan-2-ylidene moieties, whereas the corresponding cyclopent-2-ylidene part of the carbanion in Figure 1 exhibits a vexing twist of 40.4° along the C-4/C-5 single bond which is even stronger than that (30.9°) in an isoelectronic imine [16]. Repulsive strain between the two 1-CH$_3$ groups and the phenyl ring may be recognized from the enlarged angle C1/C2/C14 = 128.7° {as also in (**1c**&THF)$_2$ [1])}, and the concomitant weak pyramidalization of C15 (= C-*ipso*) is clearly visible in Figure 1. However, the rotational orientation of the phenyl group is almost orthogonal (ca. 85°) with respect to the C2/C14 double bond, thus providing for a nearly optimum overlap of the σ-type carbanionic electron pair at C-α (= C14, as shown in Scheme 1) with the aromatic π system [17]. Each THF ligand has one of its OCH$_2$ protons close to one of the six 3-CH$_3$ protons (distance down to 2.3 Å) or to one of the two aromatic *ortho*-protons (2.6 Å). The two oxygen atoms are in a trans relation at the Li$_2$C$_2$ core with angles of O1/Li1/Li1A = 163.2°.

The various short distances [13] were essentially retained when the crystals of (**2a**&THF)$_2$ were dissolved in [D$_8$]toluene, as established by two-dimensional interproton NOESY experiments at 25 °C. At –70 °C (Figure 2), the six-proton NMR singlet of 3-CH$_3$ was broadened by the adjacent Li cations, whereas the six-proton singlet of 1-CH$_3$ remained sharp. Ultimate evidence for the dimeric nature of this dissolved species was obtained at –70

°C (Figure 3) through a 1:2:3:2:1 quintet splitting of the ^{13}C-α NMR resonance with $^{1}J_{C,Li}$ = 7.5 Hz, as anticipated for the disolvated (d = 1) CLi_2 motif in the Introduction. Because this splitting pattern did not change over the temperature range of –96 to –15 °C (Table S12 [13]), one can dismiss the possible structure of a higher cyclooligomer which would have displayed the contracted "fluxional" ^{13}C-α multiplet that would result through intraaggregational scrambling of more than two Li cations [9] on warming up. Therefore, the persistent splitting pattern established that the disolvated solid-state topology of (**2a**&THF)$_2$ had passed over to the [D_8]toluene solution. Importantly, the ^{1}H and ^{13}C NMR OCH_2 signals of THF broadened on cooling and split at –96 °C into separate absorptions for OCH_2 of coordinating and free THF (for instance, δ_C = 69.0 and 67.9 ppm, respectively). Although these absorptions (Figures 4 and 5) were not baseline-separated, the signal area assigned to coordinated OCH_2 was compatible with d = 1 in (**2a**&THF)$_2$.

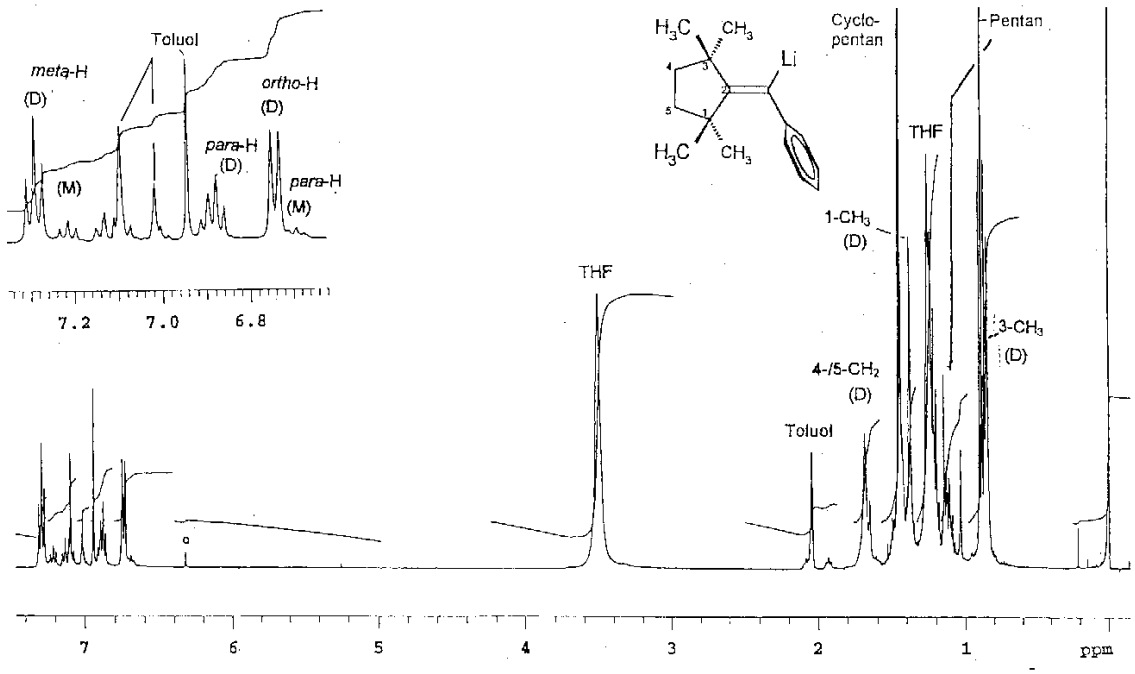

Figure 2. ^{1}H NMR spectrum (400 MHz, –70 °C) of **2a** and THF (2.6 equiv) in [D_8]toluene; M = monomer, D = dimer, o = olefin **9a**.

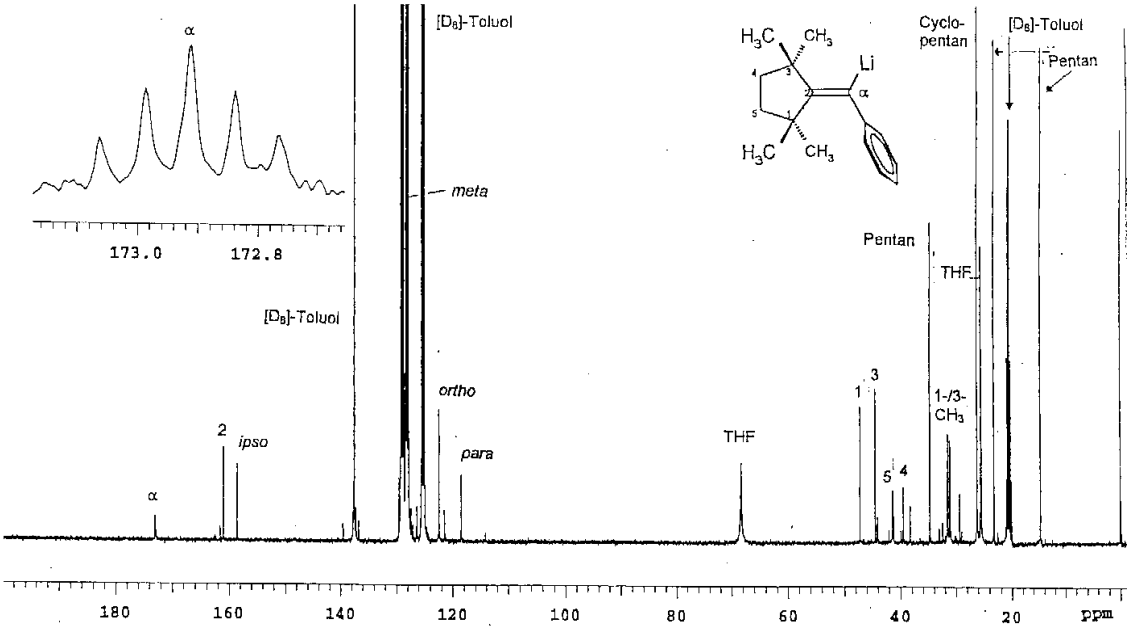

Figure 3. ^{13}C NMR spectrum (100.6 MHz, –70 °C) of dimeric **2a** and THF (2.6 equiv) in [D_8]toluene. Insert: C-α as a quintet with $^{1}J_{C,Li}$ = 7.5 Hz; o = olefin **9a**.

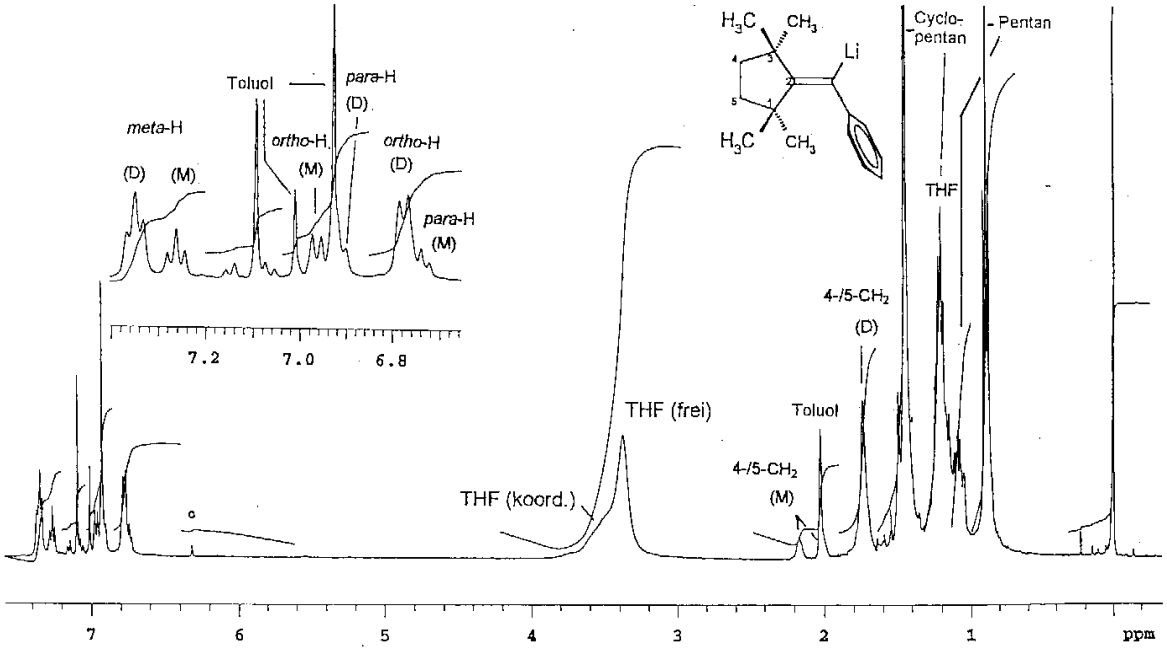

Figure 4. THF signal splitting in the ^{1}H NMR spectrum (400 MHz, –96 °C) of **2a** and THF (2.6 equiv) in [D_8]toluene; M = monomer, D = dimer, o = olefin **9a**, frei = free, koord. = coordinated. Compare M and D with Fig. 2.

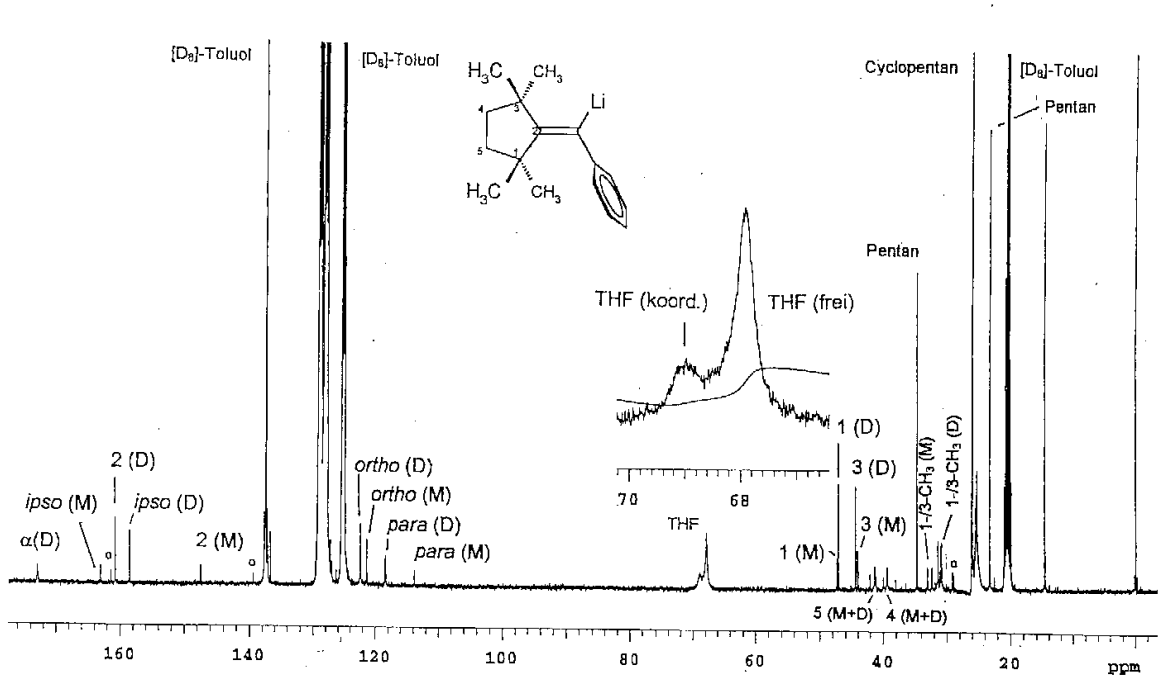

Figure 5. THF signal splitting in the ^{13}C NMR spectrum (100.6 MHz, –96 °C) of **2a** and THF (2.6 equiv) in [D_8]toluene; M = monomer, D = dimer, o = olefin **9a**, frei = free, koord. = coordinated. Compare M and D with Fig. 3.

An increasing portion of trisolvated, monomeric **2a** emerged in this [D_8]toluene solution (Tables S9 and S12 [13]) at temperatures below –32 °C (up to 28% at –96 °C in Figures 4 and 5, to be compared with Figures 2 and 3, respectively), which established the deaggregation of (**2a**&THF)$_2$ to be exothermic (and the reverse dimerization of monomeric **2a** to be endothermic) in agreement with previous evidence [2] for **1a** and **1c**. Although this monomeric component of **2a** in toluene did not exhibit a resolved $^1J_{C,Li}$ splitting, it was identified by its other NMR data (Tables S9 and S12 [13]) which closely resembled those of monomeric **2a**&3THF in THF as the solvent (Figures 6 and 7). The latter monomeric contact ion pair (CIP with $n = a = 1$) was recognized at –82 °C in THF (Figrure 7) by virtue of its ^{13}C-α triplet (1:1:1) splitting, and its microsolvation by $d = 3$ THF ligands followed from the magnitude of $^1J_{C,Li}$ = 10.7 Hz, as anticipated in the Introduction. Therefore, the

ground-state of **2a**&3THF cannot be a solvent-separated ion pair (SSIP) since that would lack the direct $^{13}C–^{6}Li$ contact. This triplet pattern was wiped out on warming to above –66 °C, because an accelerating C–Li bond breaking destroyed the $^{13}C,^{6}Li$ spin coherence, whereas all aromatic resonance positions did not change significantly between –82 and +55 °C (Tables S7 and S10 [13]), which established the presence of a sole species (namely, monomeric **2a**) all over this range. On further warmup, the accelerating cis/trans stereoinversion led to NMR line-broadening and signal coalescences of the aliphatic nuclei as analyzed in the sequel. However, the above-mentioned monomeric portion of **2a**&3THF in [D_8]toluene (Tables S9 and S12) showed no significant line broadening (hence no signs of a rapid cis/trans stereoinversion) [13].

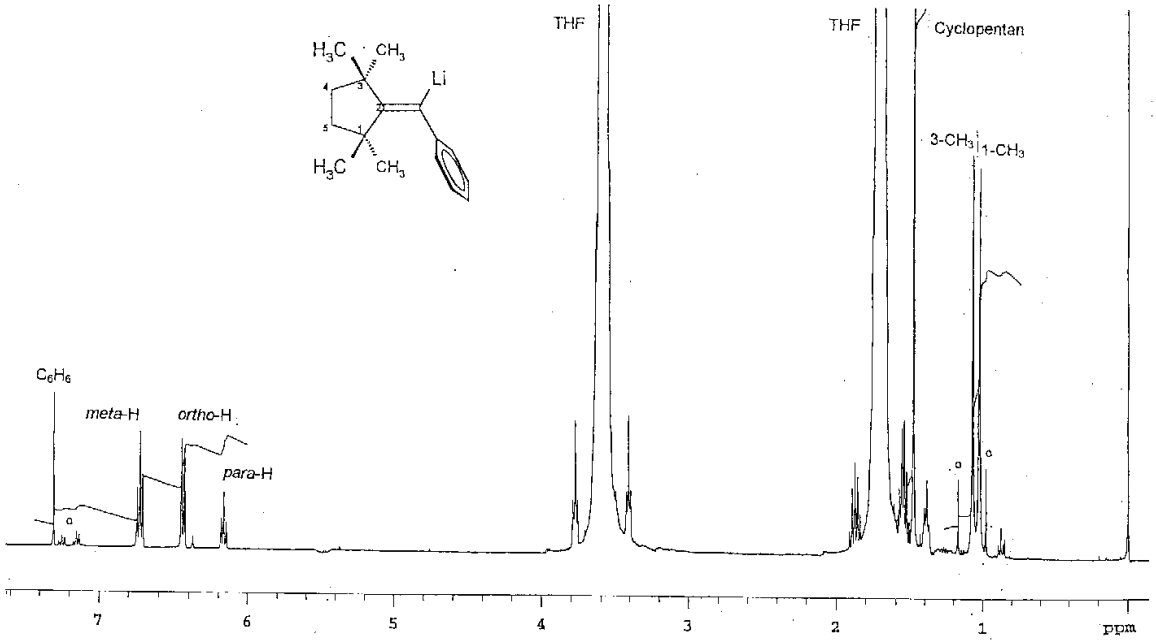

Figure 6. ^{1}H NMR spectrum (400 MHz, –66 °C) of monomeric **2a** in THF; o = olefin **9a**.

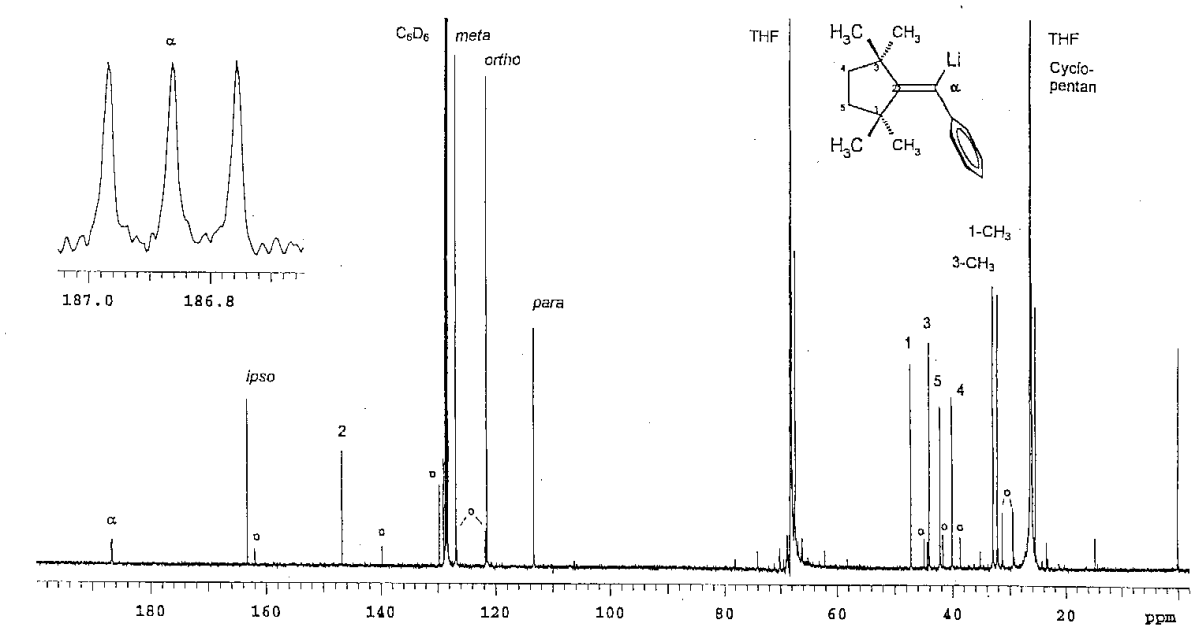

Figure 7. ^{13}C NMR spectrum (100.6 MHz, –66 °C) of monomeric **2a** in THF; o = olefin **9a**. Insert: C-α as a triplet with $^{1}J_{C,Li}$ = 10.7 Hz at –82 °C.

*2.2. The pseudomonomolecular, ionic sp^2-stereoinversion of **2a** in THF*

The cis/trans stereoinversion of the monomer **2a**&3THF, depicted in Scheme 3 as an interconversion of the CIP ground-states **10** and **10´**, cannot proceed over the very high energy barrier that opposes a simple rotational motion of the C-2/C-α double bond. Instead, a transitory cleavage of the C–Li bond is necessary in order to provide for migration of the lithium cation during stereoinversion of the carbanion. The rapidity of this diastereotopomerization [18] became perceptible on the NMR time scales (400 and 100.6 MHz, Tables S7 and S10 [13]) through coalescences of the NMR signals of pairwise interconverting diastereotopic (namely, constitutionally but not stereochemically equivalent) ^{1}H and ^{13}C nuclei: 1-C*H*$_3$/3-C*H*$_3$ at –20 °C, 1-*C*H$_3$/3-*C*H$_3$ at –5 °C, *C*H$_2$-5/*C*H$_2$-4 at +25 °C, and C-1/C-3 at +40 °C.

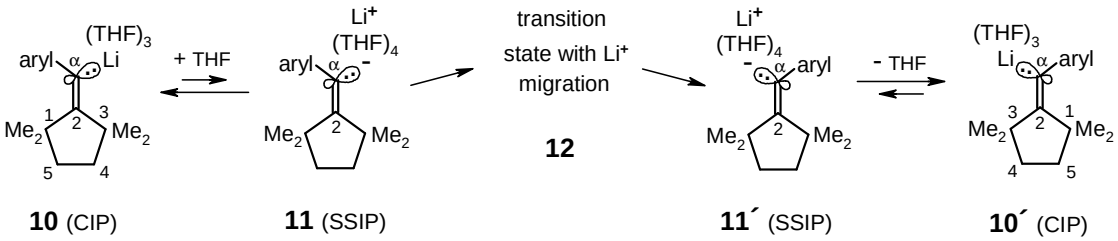

Scheme 3. Proposed mechanism of sp^2-stereoinversion of the monomeric contact ion pairs (CIP) **10** and **10´** of **2a**&3THF and **2b**&3THF.

Full line shape analyses [19] of the broadened NMR signals furnished the pseudo-first-order rate constants k_ψ of stereoinversion as a function of the temperature: As shown in Figure 8, these k_ψ values (Table S1 [13]) do not depend on the concentration of the monomer **2a**&3THF. This excludes the possibility of a bimolecular stereoinversion mechanism via an aggregated intermediate; it excludes also a dissociative ionic mechanism via the free ions. It leaves the possibility of a nondissociative ionisation with the transitory formation of an NMR-invisible amount of a solvent-separated ion pair **11** (SSIP); in this intermediate, the required C–Li bond heterolysis is accomplished at the expense of the usual immobilisation of solvent at lithium. Since the ground-state **10** of **2a**&3THF is already trisolvated, only one further THF molecule needs to be "frozen" to generate $Li^+(THF)_4$ in **11** with a corresponding entropy contribution of ca. -11 cal mol^{-1} K^{-1} as delineated in ref [2]. After migration of $Li^+(THF)_4$ on the way to the transition state **12** and beyond with formation of **11´** (SSIP) in Scheme 3, one of the four THF ligands will be released to generate the product **10´** of stereoinversion, so that the total process is pseudomonomolecular, namely, monomolecular (kinetically of first order) in the monomer **2a**&3THF and catalyzed by free THF. Thus, the measured pseudo-first-order rate constants $k_\psi = k_o$[free THF] are the products of the "true" second-order rate constants k_o and the concentrations of free THF. We did not strive for an experimental confirmation of this kinetically first-order catalysis by THF because a significant (at least 2-fold) decrease of the concentration [free THF] would entail a serious change of the

solvent polarity with questionable kinetic evidence. As previously [10] with **1a**&3THF, we prefer to leave the constant factor of [free THF] latent in k_ψ, admitting that the "true" activation entropy $\Delta S^\ddagger$ (as derived from the k_o data) would be more negative than the measured pseudoactivation entropy of $\Delta S_\psi^\ddagger = -23.3$ cal mol^{-1} K^{-1} (from k_ψ) by a mathematical correction of roughly [2] $R \times \ln$[free THF] = ca. 5 cal mol^{-1} K^{-1} (where R = 1.986 cal mol^{-1} K^{-1}).

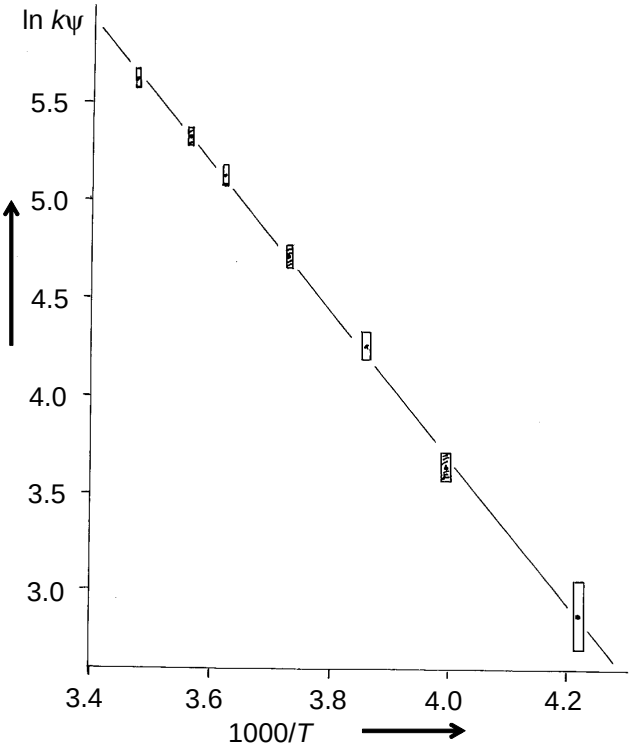

Figure 8. Arrhenius diagram of the natural logarithms of pseudo-first-order sp^2-stereoinversion rate constants k_ψ [s^{-1}] versus 1000/T [K^{-1}] for **2a** in THF as the solvent. Concentrations of **2a**: open symbols, 0.13 M; hatched, 0.06 M.

The pseudomonomolecular, ionic mechanism of **2a** and **2b** in Scheme 3 is an independently deduced example of the sp^2-stereoinversion pathway that had been established [10] for monomeric **1a** and **1b**. Even the numerical values of the pseudoactivation parameters $\Delta H_\psi^\ddagger$ (enthalpy), $\Delta S_\psi^\ddagger$ (entropy), and $\Delta G_\psi^\ddagger$ (0 °C) = $\Delta H_\psi^\ddagger - (273\text{ K}) \times \Delta S_\psi^\ddagger$ (free enthalpy) of **2a**

(entry 1 in Table 1) are almost identical with those of **1a** (entry 2). Therefore, the conclusions to be drawn for **2a** should be similar to those presented earlier [10] for **1a**, for which we established "the temporary development of considerably more negative π-charge density in the 4´-position" of the α-aryl substituent in the transition state of stereoinversion. In particular, the obvious absence of a kinetic influence of the obstructive benzo part of **1a** (as compared with **2a**) appears to support the suggestion [10] that "$Li^+(THF)_4$ migrates along the charge gradient" (C-*meta* → C-*para*) that was shown to increase on the way to the transition state.

Table 1. Pseudoactivation parameters $\Delta G_{\psi}^{\ddagger}$ (kcal mol^{-1} at 0 °C), $\Delta H_{\psi}^{\ddagger}$ (kcal mol^{-1}), and $\Delta S_{\psi}^{\ddagger}$ (cal mol^{-1} K^{-1}) of cis/trans diastereotopomerization rates of the trisolvated, monomeric 1-aryl-1-alkenyllithiums **1** and **2** in THF, and ^{13}C,^{6}Li coupling constants ^{1}J.

entry	cpd. no.	aryl substituent	$\Delta G_{\psi}^{\ddagger}$(0 °C)	$\Delta H_{\psi}^{\ddagger}$	$\Delta S_{\psi}^{\ddagger}$	^{1}J (Hz)	reference
1	**2a**	*p*-H	13.259 ± 0.002	6.91 ± 0.25	–23.3 ± 0.9	10.7	this work
2	**1a**	*p*-H	13.35 ± 0.03	6.63 ± 0.24	–24.6 ± 1.0	10.7	[10]
3	**2b**	*o*,*o*´-Me$_2$	12.71 ± 0.02	6.87 ± 0.14	–21.4 ± 0.6	10.7	this work
4	**1b**	*o*,*o*´-Me$_2$	12.47 ± 0.01	6.77 ± 0.18	–20.8 ± 0.7	10.7	[10]

2.3. Synthesis and properties of alkenyllithium ***2b***

The known [20] α-chloroalkene **13** (Scheme 4) and *n*BuLi in THF generated *n*BuCl and the alkenyllithium **2b** within ca. two hours at r.t. (or at –4 °C with a first half-life time of ca. 75 min). Unfortunately, **2b** and *n*BuCl recombined at a comparable rate to give LiCl and the α-butyl product **15c** along with the "parent" olefin [21] **15a** (ca. 2:1). This Cl/Li interchange reaction of **13** in THF was faster at –70 °C with *t*BuLi, of which a second equivalent was applied as usual [22] in the hope of destroying the coproduct *t*BuCl. Regrettably, the formation of alkenyllithium **2b** and its protonation by *t*BuCl (affording **15a**) also occurred at comparable rates and in competition with the intended proton transfer from *t*BuCl to *t*BuLi, so that only ca. 30% of **2b** survived, as shown through trapping with $ClSnMe_3$ (providing **14**) or with D_2O which furnished **15a** and **15b** (7:3). The similar generation of **2b** from **13** and *t*BuLi in *t*BuOMe as the solvent did not take place at –70 °C but was complete at r.t. within 10 minutes: A major portion of **2b** was again protonated by *t*BuCl, while the surviving portion could be observed (^{1}H NMR) in situ at r.t. and was trapped with $ClSnMe_3$ or, after 4.5 hours at r.t., with solid CO_2 to afford **15a** and the acid **15d**. The reaction of **13** with *n*BuLi in *t*BuOMe required many hours at r.t., producing **2b** and *n*BuCl which coupled more slowly to give **15c** and **15a**. All of these observations illustrate the impeding influence of steric congestion in **13** or in **2b** on the attack by nucleophiles (R–Li) or electrophiles (*n*BuCl or *t*BuCl), respectively, in ethereal solvents.

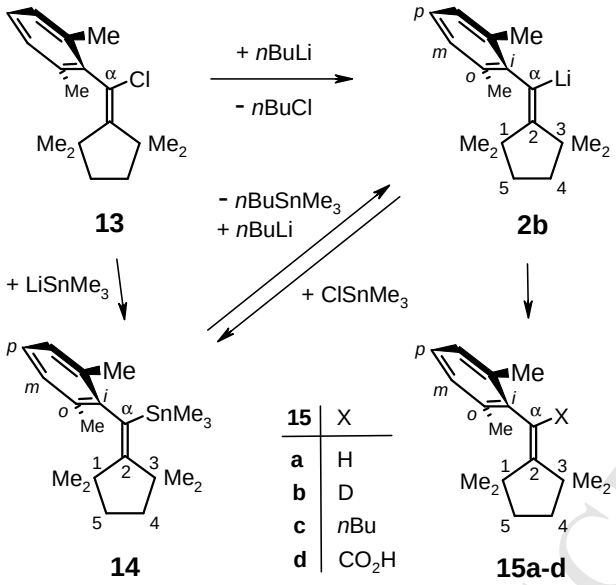

Scheme 4. Preparation and derivatives of **2b**.

The recommendable method of preparing the α-$SnMe_3$ derivative **14** from **13** used $LiSnMe_3$ in THF [15] at r.t. Well-resolved $^{1}H,^{119}Sn$ couplings were detected for the 3-CH_3 (ca. 3 Hz [23]) and the *o,o´*-CH_3 protons in **14** (4.4 Hz = ^{5}J or through space?), whereas such long-range coupling was not observed for 1-CH_3 (^{5}J) and 1-*C*H_3 (^{4}J). Pure **14** and *n*BuLi in THF produced the alkenyllithium **2b** and *n*$BuSnMe_3$ at 35 °C within less than two minutes. In contrast to the behavior of **6** (Scheme 2), this Li/Sn interchange reaction occurred neither in *t*BuOMe (slow formation of MeLi only) nor in Et_2O; but it proceeded within 72 hours at r.t. in Et_2O containing one equivalent of THF, accompanied by some deterioration that furnished the olefin **15a**. Therefore, **2b** could not be crystallized and purified (like **2a**) for studies with donor molecules other than THF. As outlined in Section 2.1 for the alkenyllithium **2a**, the 1:1:1 triplet splitting of ^{13}C-α (Figure 9) identified the monomeric state of [^{6}Li]**2b** in THF as the solvent below –59 °C, while the microsolvation number $d = 3$ followed through eq 1 from the magnitude of the NMR coupling constant $^{1}J_{C,Li} = 10.7$ Hz with the same sensitivity factor of $L = 42$ that was used before. As an independent confirmation of trisolvation in THF, Scheme 5 compares lithiation NMR shifts $\Delta\delta = \delta(R–Li) – \delta(R–H)$ for **2b** (**16**) and the

bona-fide monomer **1b**&3THF (**17**) [24]. Because $\Delta\delta$ data are known [1] to be clearly different for tri- and disolvated monomers and disolvated dimers and the unsolvated trimer of the indan-2-ylidene family [25] that includes **1a** and **1b**, the closely similar values for comparable positions in **16** and **17** certified the proposed structure of **2b**&3THF. This monomer remained the only detectable species of **2b** in THF between –85 and +25 °C, as shown (Tables S8 and S11 [13]) by the practically temperature-independent chemical shift values of the aromatic ^{1}H and ^{13}C nuclei that do not participate in the cis/trans diastereotopomerization. As all of the diastereotopic atoms belong to the cyclopent-2-ylidene part of **2b**, their NMR signals (Figures 9 and 10) tended to be disturbed by the aliphatic contaminations which could not be removed since **2b** did not crystallize. Therefore, only the C-4/C-5 and 1-CH_3/3-CH_3 pairs of ^{13}C nuclei proved suitable for line shape analyses [19] of sp^2-stereoinversion at merely four temperatures and only one concentration (Table S2 [13]). Nevertheless, the resulting pseudoactivation parameters of **2b** (entry 3 of Table 1) and their error limits were very similar to those of **1b** (entry 4), suggesting once more that migration of $Li^+(THF)_4$ in the transition state is hardly influenced by the obstructive benzo part of **1b** which is absent in **2b**. The free pseudoactivation enthalpies $\Delta G_\psi^{\ddagger}$ (0 °C) revealed that **2b**&3THF inverts a little faster than **2a**&3THF, perhaps due to a somewhat lower internal mobility (less negative activation entropy) in the ground-state of **2b**.

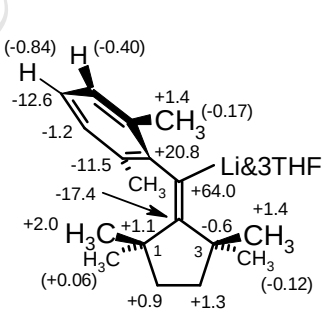

16: **2b** in THF, -85 ℃

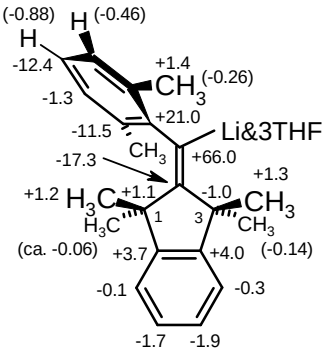

17: **1b** in THF, -95 ℃

Scheme 5. Lithiation shifts $\Delta\delta = \delta(R–Li) – \delta(R–H)$ for ^{13}C and (in parentheses) ^{1}H NMR signals of the trisolvated monomers **2b** and **1b** in THF as the solvent.

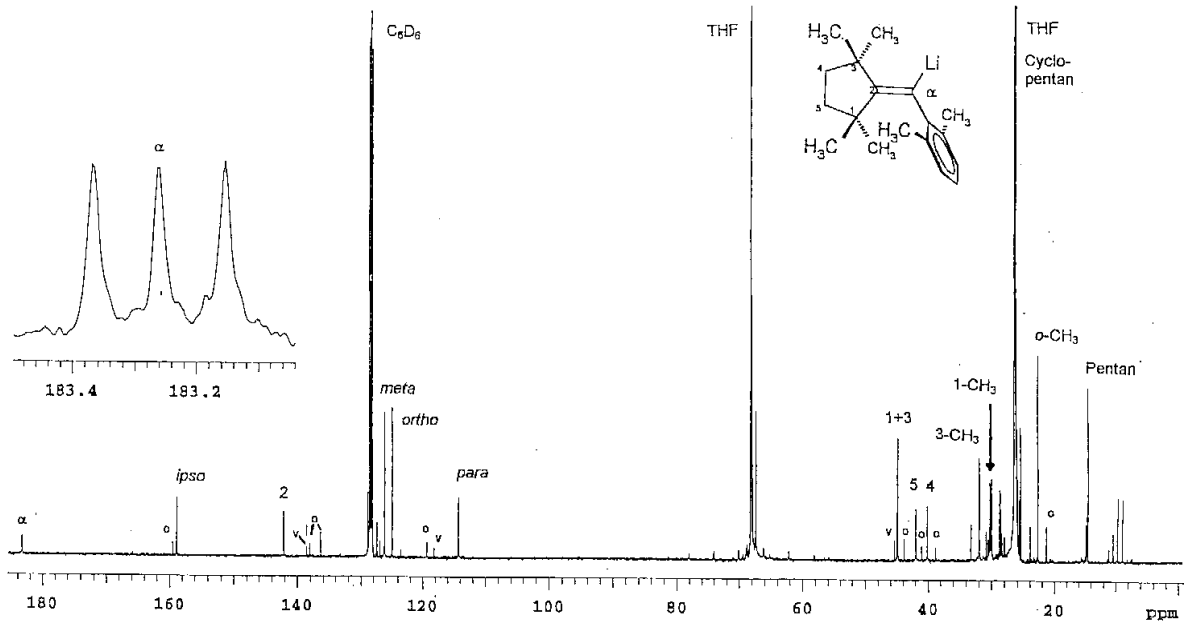

Figure 9. ^{13}C NMR spectrum (100.6 MHz, –85 °C) of monomeric **2b** in THF; o = olefin **15a**, v = contamination. Insert: C-α as a triplet with $^{1}J_{C,Li}$ = 10.7 Hz at –85 °C.

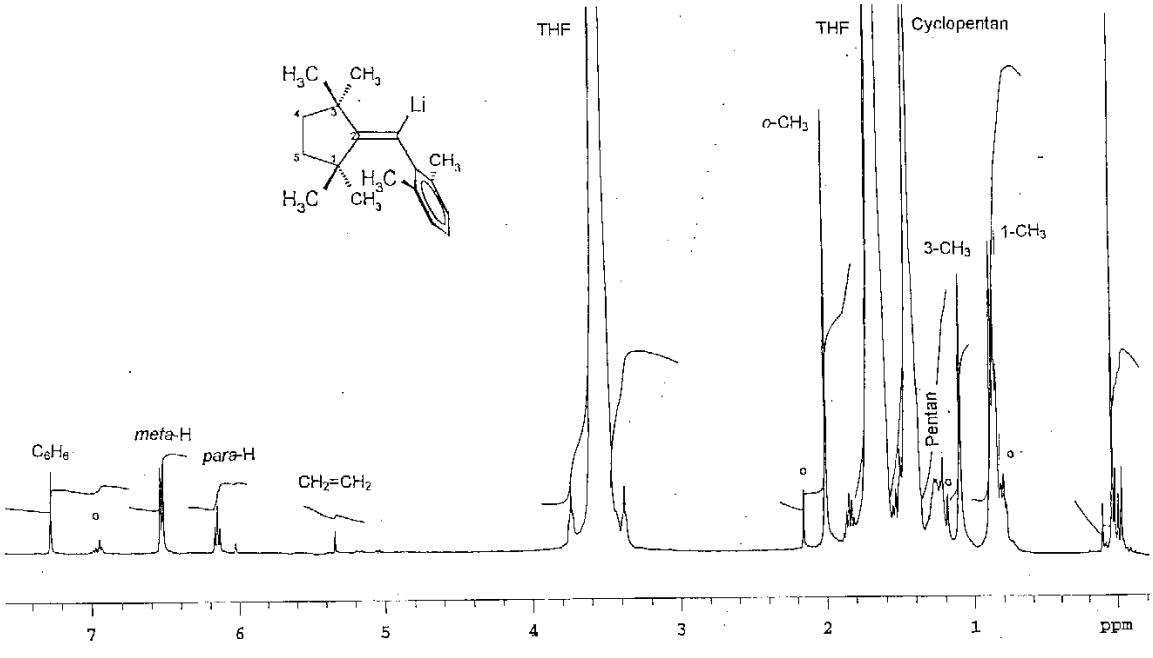

Figure 10. ^{1}H NMR spectrum (400 MHz, –85 °C) of monomeric **2b** in THF; o = olefin **15a**.

3. Conclusion

The pseudomonomolecular, ionic sp^2-stereoinversion mechanism was established for two new examples (**2a**,**b**) in THF as the solvent through some of the criteria that had been shown [10] to provide conclusive evidence for **1a** and **1b**: (i) the $^{1}J(^{13}\text{C-}\alpha,^{6}\text{Li})$ magnitudes and splitting patterns characterize monomeric, trisolvated CIP ground-states of **2a** and **2b**; (ii) the concentration–independent pseudo-first-order rate constants of sp^2-stereoinversion exclude both bimolecular and dissociative mechanisms for **2a**; (iii) the strongly negative pseudoactivation entropies $\Delta S_{\psi}^{\ddagger}$ of **2a** and **2b** resemble those of **1a** and **1b** (Table 1). This points as previously [10] to nondissociative ionization via an SSIP intermediate with THF catalysis through immobilization of only one THF ligand as the common cause, inclusive of a similar entropic penalty of a ca. 49% portion of the measured $\Delta S_{\psi}^{\ddagger}$ values of ca. –23 cal mol^{-1} K^{-1}. The inherent kinetic privilege [10] of THF over Et_2O is confirmed by an extrapolation of the rate constants of **2a** to –55 °C that yields a pre-inversion life time of ca. 0.16 seconds in THF, to be compared to > 1800 seconds reported [26] for the $Z \rightarrow E$ stereoinversion of **18** to give **19** (Scheme 6) in Et_2O as the solvent at –55 °C.

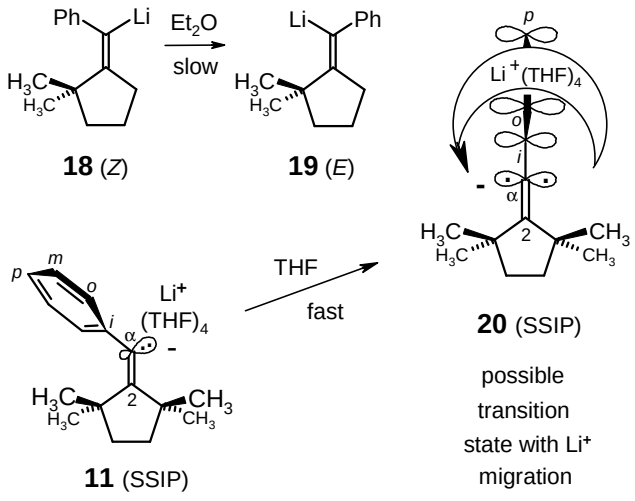

Scheme 6. Slow $Z \rightarrow E$ interconversion of **18** in Et_2O [26]; proposed transition state **20** of the much faster cis → trans sp^2-stereoinversion via the SSIP intermediate **11** in THF.

Compared with their more backside-shielded benzo relatives **1a** and **1b**, the two new examples (**2a**,**b**) perform the stereoinversion in THF with almost the same enthalpy barriers, respectively. This suggested that the migration of $Li^+(THF)_4$ was not influenced by the benzo moiety in **1** but occurred along the π-charge gradient within the α-aryl substituents that is roughly illustrated by the Δδ values of **16** in Scheme 5 and intensifies [10] on the way to the transition state **20**.

4. Experimental

4.1. General remarks

Organolithium samples were prepared and handled under a stream of dry argon cover gas as detailed in ref [1]. Pseudo-first-order stereoinversion rate constants k_ψ were determined as described in ref [10]. All ^1H and ^{13}C NMR chemical shifts are referenced to internal TMS.

*4.2. 2-(α-Lithiobenzylidene)-1,1,3,3-tetramethylcyclopentane (**2a**)*

A dry NMR tube (5 mm) was charged under argon cover gas at r.t. with the stannyl compound **6** (70 mg, 0.19 mmol), dry pentane (0.50 mL), anhydrous THF (0.047 mL, 0.57 mmol), and after short mixing finally with [^{6}Li]*n*BuLi (0.54 mmol) [27] in cyclopentane (0.31 mL). The tube was closed with a soft rubber stopper that was wrapped with a layer of parafilm®. After gentle tilting without wetting the stopper, the tube was kept overnight at 22 °C under argon cover gas in a big Schlenk tube for completion of the Li/Sn interchange reaction. On subsequent cooling to 2 °C for five hours, the first crystals appeared after ca. 80 min and grew over the next three hours. The tube was then cooled at –70 °C for 15 min, whereupon the supernatant was withdrawn by syringe. The block-shaped crystals were

suspended in dry cyclopentane (0.3 mL) at r.t. and re-cooled at –70 °C during the withdrawal of this supernatant. After further three of such washing procedures, these crystals of (**2a**&1THF)$_2$ were stored under cyclopentane in an inclined-lying, big Schlenk tube filled with argon gas at –18 °C. For NMR measurements, the cyclopentane was withdrawn and the colorless crystals were blown dry in a stream of dry argon gas at r.t. for five seconds, then finally cooled under argon to –70 °C and dissolved in an anhydrous solvent (Tables S7, S9, S10, and S12 [13]). ^{1}H NMR of the monomer **2a**&3THF (THF, –82 °C, 400 MHz) δ 1.03 (s, 6H, 2 × 1-CH$_3$), 1.07 (s, 6H, 2 × 3-CH$_3$), 1.39 (t, 2H, CH$_2$-5 or CH$_2$-4), 6.17 (t, 1H, ^3J 7.0 Hz, *p*-H), 6.44 (d, 2H, ^3J 8.0 Hz, 2 × *o*-H), 6.73 (t, 2H, ^3J 7.5 Hz, 2 × *m*-H) ppm, assigned through comparison with monomeric **1a**&3THF [1]; ^{1}H NMR of the monomer **2a**&3THF ([D$_8$]toluene, –70 °C, 400 MHz) δ 1.43 (s, 6H, 2 × 1-CH$_3$), 1.65 (s, 6H, 2 × 3-CH$_3$), 1.93 (t, 2H, CH$_2$-5), 2.08 (t, 2H, CH$_2$-4), 6.69 (t, 1H, ^3J 7.4 Hz, *p*-H), 6.90 (d, 2H, 2 × *o*-H), 7.21 (t, 2H, ^3J 7.5 Hz, 2 × *m*-H) ppm; ^{1}H NMR of the dimer (**2a**&1THF)$_2$ ([D$_8$]toluene, 25 °C, 400 MHz) δ 0.85 (broadened s, 6H, 2 × 3-CH$_3$), 1.26 (sharp s, 6H, 2 × 1-CH$_3$), 1.60 (m, 2H, CH$_2$-5), 1.63 (m, 2H, CH$_2$-4), 6.67 (d, 2H, ^3J 7.5 Hz, 2 × *o*-H), 6.75 (t, 1H, ^3J 7.3 Hz, *p*-H), 7.14 (t, 2H, ^3J 7.5 Hz, 2 × *m*-H) ppm, assigned through the NOESY correlations (25 °C) *p*-H ↔ *m*-H ↔ *o*-H (the only two-proton doublet) ↔ 1-CH$_3$ ↔ 5-H, and 1-CH$_3$ ↔ OCH$_2$ of THF ↔ 3-CH$_3$; ^{13}C NMR of the monomer **2a**&3THF (THF, –82 °C, 100.6 MHz) δ 32.1 (2 × 1-CH$_3$), 32.9 (2 × 3-CH$_3$), 40.1 (CH$_2$-4), 42.2 (CH$_2$-5), 44.0 (C-3), 47.2 (C-1), 113.3 (C-*p*), 121.4 (2 × C-*o*), 126.8 (2 × C-*m*), 146.6 (C-2), 163.2 (C-*ipso*), 186.9 (t, $^1J_{C,Li}$ 10.7 Hz, C-α) ppm, assigned through comparison with monomeric **1a**&3THF [1]; ^{13}C NMR of the monomer **2a**&3THF ([D$_8$]toluene, –83 °C, 100.6 MHz) δ 32.4 (2 × 1-CH$_3$), 33.1 (2 × 3-CH$_3$), 40.0 (CH$_2$-4), 42.0 (CH$_2$-5), 44.1 (C-3), 47.3 (C-1), 113.9 (C-*p*), 121.4 (2 × C-*o*), 127.2 (2 × C-*m*), 147.7 (C-2), 162.9 (C-*ipso*), 185.2 (broad, C-α) ppm; ^{13}C NMR of the dimer (**2a**&1THF)$_2$

([D_8]toluene, 25 °C, 100.6 MHz) δ 31.64 (sharp q, 2 × 1-CH_3), 31.68 (broadened q, 2 × 3-CH_3), 39.8 (tm, ^1J 127.5 Hz, CH_2-4), 41.9 (tm, ^1J 127.5 Hz, CH_2-5), 44.4 (m, C-3), 47.3 (m, C-1), 118.5 (broadened d, ^1J 158 Hz, C-*p*), 122.7 (broadened d, ^1J 153 Hz, 2 × C-*o*), 128.3 (obscured dd, ^1J ca. 153 Hz, 2 × C-*m*), 158.6 (broadened t, ^3J ca. 6 Hz, C-*ipso*), 161.6 (very broad, C-2), 173.3 (very broad, C-α) ppm, assigned through HSQC and the following two-dimensional $^2J_{C,H}$ and $^3J_{C,H}$ correlations (25 °C, window 6 Hz): 1-*C*H_3 ↔ 1-C*H*$_3$ ↔ *C*H_2-5, *C*H_2-4 ↔ 3-C*H*$_3$ ↔ C-3 ↔5-H ↔ 1-*C*H_3, and 1-C*H*$_3$ ↔ C-1; ^{13}C NMR of the dimer (**2a**&1THF)$_2$ ([D_8]toluene, –83 °C, 100.6 MHz) δ 31.0 (2 × 3-CH_3), 31.5 (2 × 1-CH_3), 39.5 (CH_2-4), 41.4 (CH_2-5), 44.4 (C-3), 47.1 (C-1), 118.4 (C-*p*), 122.4 (2 × C-*o*), 128.4 (2 × C-*m*), 158.5 (C-*ipso*), 160.9 (C-2), 172.9 (sharp qi, $^1J_{C,Li}$ 7.5 Hz, C-α) ppm. For further NMR data, see Tables S7, S9, S10 and S12 [13].

A similar procedure with unlabeled *n*BuLi furnished the colorless, block-shaped single crystal that precipitated from pentane at –20 °C and was washed only once with pentane for the X-ray diffraction analysis at –100 °C.

*4.3. 2-(α-Lithio-o,o´-dimethylbenzylidene)-1,1,3,3-tetramethylcyclopentane (**2b**)*

The α-stannyl precursor **14** (50 mg, 0.123 mmol), anhydrous THF (0.50 mL), and [D_6]benzene (0.080 mL) were placed in a dry NMR tube (5 mm) and cooled to –70 °C under argon gas cover for the addition of [^{6}Li]*n*BuLi (0.185 mmol) in cyclopentane (0.11 mL). The tube was closed with a soft rubber stopper, sealed with parafilm,® shaken gently for 5 min at r.t., and stored at –70 °C in a big Schlenk tube filled with argon gas. This THF solution of monomeric **2b**&3THF (Tables S8 and S11 [13]) will deteriorate within 60 min at 35 °C with formation of the "parent" olefin **15a**. We did not succeed in crystallizing **2b** or studying it in other solvents. ^{1}H NMR (THF, –85 °C, 400 MHz) δ 0.93 (s, 6H, 2 × 1-CH_3), 1.14 (s, 6H, 2 × 3-CH_3), 2.06 (s, 6H, 2 × *o*-CH_3), CH_2-5 and CH_2-4 overlaid, 6.20 (t, 1H, ^3J 7.0 Hz, *p*-H), 6.58 (d, 2H, ^3J 7.0 Hz, 2 × *m*-H) ppm, assigned through comparison with monomeric **1b**&3THF

[10]; ^{13}C NMR (THF, –85 °C, 100.6 MHz) δ 22.6 (2 × *o*-CH_3), 30.0 (2 × 1-CH_3), 31.9 (2 × 3-CH_3), 40.1 (CH_2-4), 41.9 (CH_2-5), 44.8 (C-3), 44.9 (C-1), 114.3 (C-*p*), 124.9 (2 × C-*o*), 126.2 (2 × C-*m*), 142.1 (C-2), 158.9 (C-*ipso*), 183.3 (t, $^1J_{C,Li}$ 10.7 Hz, C-α) ppm, assigned as above.

*4.4. 1-(α-Bromobenzyl)-2,2,5,5-tetramethylcyclopentanol (**4**)*

A round-bottomed flask (1000 mL) was charged with 1-benzyl-2,2,5,5-tetramethylcyclopentanol [12] (**3**, 15.00 g, 64.55 mmol), *N*-bromosuccinimide (NBS, 17.30 g, 96.8 mmol), CCl_4 (500 mL), azobis(isobutyronitrile) (AIBN, 1.65 g, 10.05 mmol), and a magnetic stirring bar. The vessel was fitted with a reflux condenser and heated up to 95 °C. A ^{1}H NMR spectrum showed 85% conversion after a reflux period of 35 min. More of NBS (3.45 g, 19.4 mmol) and AIBN (500 mg, 3.04 mmol) was added and refluxing continued with stirring for 30 min at 95 °C. This controlled addition served to avoid overbromination that would have formed the α,α-dibromide with a very rapidly ensuing ring expansion. After cooling in an ice bath, the supernatant succinimide powder was removed by filtration, and the solvent was distilled off in a rotary evaporator without heating to leave crude **4** as a yellow liquid (22.7 g) which should immediately be processed to give **5** before the slower ring expansion of **4** would form the ketone **8**. ^{1}H NMR of **4** (CCl_4, 80 MHz) δ 0.33, 0.93, 1.28, and 1.46 (4 s, 4 × 3H, 4 × CH_3), ca. 1.71 (overlaid m, 2 × CH_2), 5.25 (s, 1H, CHBr), 7.19 (m, 5H, phenyl) ppm.

*4.5. 2-(α-Bromobenzylidene)-1,1,3,3-tetramethylcyclopentane (**5**)*

The crude 1-(α-bromobenzyl)-2,2,5,5-tetramethylcyclopentanol (**4**, 22.7 g, maximum 64.55 mmol) was dissolved in distilled pyridine (175 mL) and cooled in an ice bath. Thionyl choride (10.0 mL, 138 mmol) was added slowly (exothermic reaction!) with stirring. After continued stirring at r.t. overnight, the black suspension was poured into aqueous HCl (2 M, 750 mL) and shaken with Et_2O (3 × 250 mL). The combined Et_2O layers were shaken with aqueous HCl (2 M, 3 ×) and washed with distilled water until neutral, then dried over Na_2SO_4

and concentrated to give crude **5** as a pale yellow liquid (15.4 g, < 81%). Pure **5** was obtained through distillation (after a forerun of white needles of AIBN, δ_H = 1.72 ppm) with bp 95–110 °C/0.004 mbar (ref [14]: 130–150 °C/1 Torr) and subsequent crystallization from small amounts of methanol at –20 °C (2 ×, mp 38–39 °C, no mp in ref [14]). ^{1}H NMR ($CDCl_3$, 400 MHz) δ 0.80 (s, 6H, 2 × 1-CH_3), 1.47 (s, 6H, 2 × 3-CH_3), 1.51 (pseudo-t, AA´ part of an AA´MM´ system, 2H, CH_2-5), 1.70 (pseudo-t, MM´ part, 2H, CH_2-4), 7.23 (m, 3H, 2 × *o*-H and overlaid *p*-H), 7.30 (tm, 2H, ^3J ca. 7 Hz, 2 × *m*-H) ppm, assigned through SCS [12] in accord with NOE difference spectra that exhibited intensification of 4-H by irradiation at {3-CH_3} and of 5-H and *o,o´*-H by {1-CH_3}; ^{13}C NMR ($CDCl_3$, 100.6 MHz) δ 26.90 (qsext, ^1J 126 Hz, ^3J 4.6 Hz, 2 × 3-CH_3), 29.00 (qsext, ^1J 126 Hz, ^3J 4.6 Hz, 2 × 1-CH_3), 41.43 (tm, ^1J ca. 127 Hz, CH_2-5), 41.45 (tm, ^1J ca. 127 Hz, CH_2-4), 47.00 (m, ^3J ca. 3.5 Hz, C-3), 47.75 (m, ^3J ca. 3.8 Hz, C-1), 115.47 (t, ^3J 4.3 Hz, C-α), 127.51 (dt, ^1J 160.6 Hz, ^3J 7.5 Hz, C-*p*), 127.77 (dd, ^1J 160 Hz, ^3J 7.5 Hz, 2 × C-*m*), 129.37 (dt, ^1J 160.5 Hz, ^3J 6.7 Hz, 2 × C-*o*), 143.31 (sharp t, ^3J 7.5 Hz, C-*ipso*), 156.85 (m, apparent ^3J ca. 4 Hz, C-2) ppm, assigned through SCS [12] in accord with selective {^{1}H} decoupling experiments as follows: {1-CH_3} → 1-*C*H_3 as a sharp t with residual ^3J to 5-H, and C-1 narrowed; {3-CH_3 and CH_2-5} → 3-*C*H_3 and *C*H_2-5 decoupled, and C-3 narrowed; IR (KBr) ν 2950, 2867, 1459, 1365, 715 (s) cm^{-1}. Anal. calcd for $C_{16}H_{21}Br$ (293.25): C, 65.53; H, 7.22; Br, 27.25. Found: C, 65.65; H, 7.17; Br, 26.56.

Alternatively, pure **5** was obtained via epoxidation of olefin **9a** [13]. **5** was not present in the complex product mixture that was formed from **9a** [12] with elemental bromine in CCl_4.

*4.6. 2-(α-Trimethylstannylbenzylidene)-1,1,3,3-tetramethylcyclopentane (**6**)*

*a) From **5** with $LiSnMe_3$.* A green solution of $LiSnMe_3$ [15] (ca. 6.14 mmol) in THF (8.77 mL) was added under argon cover gas to the bromoalkene **5** (1.00 g, 3.41 mmol) in anhydrous THF (4 mL) with stirring at –72 °C. The mixture was stirred for another 15 min and then at

r.t. for 45 min, poured onto solid CO_2, warmed up, diluted with 2 M aqueous NaOH (25 mL), and shaken with Et_2O (3 × 10 mL). The combined Et_2O extracts were washed with distilled water until neutral, dried over Na_2SO_4, and concentrated to give a yellowish mixture (1.27 g) of **6**, olefin **9a**, and Sn_2Me_6 (6:2:2). Microdistillation separated **9a** [bp 86–92 °C (bath temp.)/0.02 mbar, 118 mg] from **6** [bp 102–118 °C (bath temp.)/0.02 mbar, 607 mg, 47% yield]; the latter fraction crystallized from ethanol at –30 °C: mp 27.5–29 °C; ^{1}H NMR ($CDCl_3$, 400 MHz) δ –0.03 (s, 9H; ^{119}Sn satellites, ^2J 51.6 Hz; α-$SnMe_3$), 0.84 (s, 6H; ^{119}Sn satellites, $|^5J| < 1.5$ Hz; 2 × 1-CH_3), 1.22 (s, 6H; ^{119}Sn satellites, ^5J (?) 3.1 Hz; 2 × 3-CH_3), 1.47 (t, 2H, ^3J 6.8 Hz, CH_2-5), 1.60 (t, 2H, ^3J 6.8 Hz, CH_2-4), 6.86 (dd, 2H, ^3J 8.2 Hz; ^{119}Sn satellites, ^4J ca. 4 Hz; 2 × *o*-H), 7.04 (tt, 1H, ^3J 7.4 Hz, ^4J 1.4 Hz, *p*-H), 7.19 (tm, 2H, ^3J 7.8 Hz, 2 × *m*-H) ppm, assigned through NOE difference spectra that exhibited intensification of CH_2-4 by irradiation at {3-CH_3} and of CH_2-5 and *o*,*o*´-H by {1-CH_3}; ^{13}C NMR ($CDCl_3$, 100.6 MHz) δ –5.23 (q; ^{119}Sn satellites, ^1J 336.5 Hz; α-$SnMe_3$), 29.91 (q; ^{119}Sn satellites, ^4J 7.6 Hz; 2 × 1-CH_3), 30.65 (q; ^{119}Sn satellites, $|^4J| \leq 4$ Hz; 2 × 3-CH_3), 40.42 (t, CH_2-5), 41.18 (t, CH_2-4), 45.22 (quart.; ^{119}Sn satellites, ^3J 21.0 Hz; C-3), 47.53 (quart.; ^{119}Sn satellites, ^3J 61.0 Hz; C-1), 124.16 (d; ^{119}Sn satellites, ^5J 12.2 Hz; C-*p*), 127.17 (d; ^{119}Sn satellites, ^4J 9.5 Hz; 2 × C-*m*), 128.47 (d; ^{119}Sn satellites, ^3J 18.7 Hz; 2 × C-*o*), 135.91 (quart.; ^{119}Sn satellites not detected; C-α), 146.00 (t, ^3J 7.2 Hz; ^{119}Sn satellites, ^2J 23.6 Hz; C-*ipso*), 167.64 (quart.; ^{119}Sn satellites, ^2J 16.6 Hz; C-2) ppm, assigned through the ^{119}Sn coupling constants and the following selective {^{1}H} decoupling experiments: {1-CH_3} → 1-*C*H_3 as a narrow t through residual coupling to CH_2, C-1 as a narrow t coupled to CH_2; {3-CH_3 + CH_2-5 + CH_2-4} → 3-*C*H_3, C-3, and *C*H_2-5 as three sharp s; IR (KBr) ν 2954, 2864, 1598, 1362, 769, 708, and 520 cm^{-1}. Anal. calcd for $C_{19}H_{30}Sn$ (377.16): C, 60.51; H, 8.02. Found: C, 61.09; H, 8.00.

*b) From **2a** with $ClSnMe_3$.* A dry Schlenk flask (25 mL) was charged with a magnetic stirring bar and *n*BuLi (3.55 mmol) in hexanes (1.42 mL) under argon cover gas. The flask

was cooled to –40 °C and treated first with anhydrous *t*BuOMe (10 mL) and then with the bromoalkene **5** (800 mg, 2.73 mmol). The resultant solution of the alkenyllithiium **2a** and residual *n*BuLi was stirred at r.t. for 20 min, whereupon $ClSnMe_3$ (707 mg, 3.55 mmol; **Caution**: very poisenous!) was added portionwise within 10 min. The mixture was stirred overnight, then poured into iced water (50 mL) and extracted with Et_2O (3 ×). The combined Et_2O extracts were washed with distilled water, dried over K_2CO_3, and concentrated to give a yellow liquid (805 mg) containing product **6** and olefin **9a** (47:53). Distilled **6** (405 mg, 39%) was stable against aqueous NaOH (2 M) or HCl (2 M) for two days (very slow formation of olefin **9a**).

*4.7. 2-Bromo-3,3,6,6-tetramethyl-2-phenylcyclohexanone (**7**)*

The colorless needles **7** were obtained (together with the monobromide **4**) through overbromination of the alcohol **3** with NBS (2.4 equiv): Mp 146–147 °C (pentane); ^{1}H NMR ($CDCl_3$, 400 MHz) δ 0.83 (s, 3H, 1 × 6-CH_3), 1.14 (s, 3H, 1 × 6-CH_3), 1.25 (s, 3H, 1 × 3-CH_3), 1.45 (ddd, 1H, $|^2J|$ 14.1 Hz, ^3J 4.2 Hz, ^3J 3.3 Hz, equat. 4-H), 1.61 (s, 3H, 1 × 3-CH_3), 1.72 (ddd, 1H, $|^2J|$ 14.1 Hz, ^3J 4.0 Hz, ^3J 3.3 Hz, equat. 5-H), 1.91 (td, 1H, $|^2J|$ 14.1 Hz, ^3J 4.2 Hz, ax. 5-H), 2.48 (td, 1H, $|^2J|$ 14.1 Hz, ^3J 4.2 Hz, ax. 4-H), 7.24–7.29 (m, 3H, 2 × *m*-H and *p*-H), 7.40 (dm, 2H, ^3J 7.2 Hz, 2 × *o*-H) ppm; ^{13}C NMR ($CDCl_3$, 100.6 MHz) δ 25.1, 27.7, and 29.3 (3 × CH_3), 33.2 and 34.2 (CH_2-4/-5), 34.5 (1 × CH_3), 41.2 and 42.8 (2 × quart., C-3/-6), 82.3 (C-2), 126.4 (2 × C-*m*), 127.5 (C-*p*), 131.3 (2 × C-*o*), 136.2 (C-*ipso*), 209.4 (C-1) ppm; IR (KBr) ν 2961, 2933, 2869, 1699 (s), 1462, 1444, 744, 702 cm^{-1}. Anal. calcd for $C_{16}H_{21}BrO$ (309.25): C, 62.14; H, 6.84; Br, 25.84. Found: C, 62.21; H, 6.76; Br, 25.88.

*4.8. 3,3,6,6-Tetramethyl-2-phenylcyclohexanone (**8**)*

See ref [13].

*4.9. 2-Benzylidene-1,1,3,3-tetramethylcyclopentane (**9a**)*

The published values and assignments [12] are correct, but the positional numbering compatible with that in the present article is as follows: ^{1}H NMR ($CDCl_3$, 400 MHz) δ 0.99 (1-CH_3), 1.17 (3-CH_3), 1.53 (CH_2-5), 1.58 (CH_2-4), 6.31 (α-H), 7.16 (*o*-H), 7.17 (*p*-H), 7.25 (*m*-H) ppm; ^{13}C NMR ($CDCl_3$, 100.6 MHz) δ 29.3 (1-CH_3), 31.1 (3-CH_3), 38.4 (CH_2-4), 41.4 (CH_2-5), 43.7 (C-1), 44.6 (C-3), 120.8 (C-α), 125.8 (C-*p*), 127.5 (C-*m*), 129.3 (C-*o*), 139.5 (C-*ipso*), 162.1 (C-2) ppm.

*4.10. α-Phenyl-α-(1,1,3,3-tetramethylcyclopent-2-ylidene)acetic acid (**9b**)*

See ref [13].

*4.11. 2-(α-Butylbenzylidene)-1,1,3,3-tetramethylcyclopentane (**9c**)*

See ref [13].

*4.12. 2-[o,o´-Dimethyl-α-(trimethylstannyl)benzylidene]-1,1,3,3-tetramethylcyclopentane (**14**)*

A solution of the chloroalkene **13** [20] (1.00 g, 3.61 mmol) in anhydrous THF (4 mL) was stirred at –70 °C under argon gas cover during the slow addition of $LiSnMe_3$ [15] (ca. 6.5 mmol) in THF (9.3 mL). This solution was stirred for at least 20 min at r.t. and then poured outo solid CO_2. After warm-up and addition of aqueous NaOH (2 M, 25 mL), the mixture was shaken with Et_2O (3 × 10 mL). The combined Et_2O layers were washed with distilled water until neutral, dried over Na_2SO_4, and concentrated to yield a solidifying oil (1.31 g) containing **14** and the olefin **15a** (7:3). A solution of this mixture in a little ethanol precipitated colorless platelets of **14** (757 mg, 52%). **14** may also be distilled at 105–120 °C (bath temp.)/0.04 mbar. Mp 96–97.5 °C (2 × from ethanol); ^{1}H NMR ($CDCl_3$, 400 MHz) δ –0.05 (s, 9H; ^{119}Sn satellites, ^{2}J 50.6 Hz; α-$SnMe_3$), 0.84 (s, 6H, 2 × 1-CH_3), 1.26 (s, 6H; ^{119}Sn satellites, ^{5}J (?) 3.3 Hz; 2 × 3-CH_3), 1.51 (pseudo-t, 2H, ^{3}J 6.8 Hz, CH_2-5), 1.58 (pseudo-t, 2H, ^{3}J 6.8 Hz, CH_2-4), 2.13 (s, 6H; ^{119}Sn satellites, ^{5}J (?) 4.4 Hz; 2 × *o*-CH_3), 6.91 (pseudo-s, 3H, 2 × *m*-H and *p*-H) ppm, assigned through the following NOE difference spectra

under selective {^{1}H} irradiation: {1-CH_3} ↔ 5-H and *o,o´*-C*H*$_3$, {3-CH_3} ↔ 4-H, {*o,o´*-CH_3} ↔ *m*-H; ^{13}C NMR ($CDCl_3$, 100.6 MHz) δ –4.09 (^{119}Sn satellites, ^1J 330 Hz; α-$SnMe_3$), 21.27 (*o,o´*-CH_3), 28.03 (^{119}Sn satellites, ^4J 8.5 Hz; 2 × 1-CH_3), 30.01 (^{119}Sn satellites, $|^4J| \leq 3.7$ Hz; 2 × 3-CH_3), 40.24 (CH_2-5), 41.00 (CH_2-4), 46.38 (^{119}Sn satellites, ^3J 23.2 Hz; C-3), 46.92 (^{119}Sn satellites, ^3J 63.4 Hz; C-1), 124.59 (^{119}Sn satellites, ^5J 12.9 Hz; C-*p*), 126.88 (^{119}Sn satellites, ^4J 9.8 Hz; 2 × C-*m*), 134.00 (^{119}Sn satellites, ^3J 19.8 Hz; 2 × C-*o*), 134.15 (^{119}Sn satellites, ^1J 453 Hz; C-α), 144.67 (^{119}Sn satellites, ^2J 15.2 Hz; C-*ipso*), 164.98 (^{119}Sn satellites, ^2J 15.6 Hz; C-2) ppm, assigned through the ^{119}Sn,^{13}C coupling constants, comparison with **6**, and the following selective {^{1}H} decoupling experiments: {*o,o´*-CH_3} → C-*o* as a d to *p*-H, C-*ipso* as a sharp t to *m,m´*-H; {1-CH_3} → 1-*C*H$_3$ as a t to C*H*$_2$-5, C-1 narrowed; {3-CH_3} → C-3 narrowed; IR (KBr) ν 2952, 1458, 1361, 764 (s), 524 cm^{-1}. Anal. calcd for $C_{21}H_{34}Sn$ (405.21): C, 62.25; H, 8.46. Found: C, 62.33; H, 8.49.

*4.13. [α-D]-2-(o,o´-Dimethylbenzylidene)-1,1,3,3-tetramethylcyclopentane (**15b**)*

The deuterium-induced isotope shifts $^n\Delta = \delta(\mathbf{15b}) - \delta(\mathbf{15a})$ across *n* bonds were measured with a worked-up 3:7 mixture of **15b** and **15a** [21] as obtained through addition of D_2O to a THF solution of **2b** that had been kept at r.t. for 15 min after its generation from the chloroalkene **13** [20] with *t*BuLi (2 equiv). ^{1}H NMR ($CDCl_3$, 400 MHz): All $|^n\Delta| < 0.001$ ppm; ^{13}C NMR ($CDCl_3$, 100.6 MHz): $^5\Delta$ = ca. +0.0109(5) for C-*p*, $^3\Delta$ = +0.0308(5) for C-*o*, $^2\Delta$ = –0.0686(5) for C-*ipso*, $^1\Delta$ = –0.334(2) and $^1J_{C,D}$ = 22.6 Hz for C-α, $^2\Delta$ = ca. –0.050(1) for C-2, $^3\Delta_{trans}$ = ca. –0.052(3) for C-1, $|^3\Delta_{cis}|$ < ca. 0.02 ppm for C-3.

*4.14. 2-(α-Butyl-o,o´-dimethylbenzylidene)-1,1,3,3-tetramethylcyclopentane (**15c**)*

See ref [13].

*4.15. α-(o,o´-Dimethylphenyl)-α-(1,1,3,3-tetramethylcyclopent-2-ylidene)acetic acid (**15d**)*

See ref [13].

Acknowledgments

Financial support of parts of this project by the Deutsche Forschungsgemeinschaft is gratefully acknowledged. We are indebted to Professor Heinrich Nöth and Dr. H. Schwenk-Kircher for performing the X-ray diffraction analysis.

Supplementary Material

1. File CyptLi1-SI.doc

Referencces

[§] *E*/*Z* Equilibria, Part 21. For Part 20, see reference [10].

[1] R. Knorr, T. Menke, K. Ferchland, J. Mehlstäubl, D. S. Stephenson, J. Am. Chem. Soc. 130 (2008) 14179–14188.

[2] R. Knorr, T. Menke, K. Ferchland, Organometallics 32 (2013) 468–472.

[3] H. J. Reich, K. J. Kulicke, J. Am. Chem. Soc. 118 (1996) 273–274, and refs quoted therein.

[4] W. Henze, A. Vyater, N. Krause, R. M. Gschwind, J. Am. Chem. Soc. 127 (2005) 17335–17342, and Figure 8a (at 239 K) therein.

[5] For example, see: G. Fraenkel, J. A. Cabral, J. Am. Chem. Soc. 115 (1993) 1551–1557.

[6] G. Fraenkel, A. M. Fraenkel, M. J. Geckle, F. Schloss, J. Am. Chem. Soc. 101 (1979) 4745–4747.

[7] For some reviews and simplified examples, see ref [1] and Chart 1 therein.

[8] See Tables 1, 2, S1, and S2 in ref [1].

[9] See ref [1] for scrambling within a cyclotrimer and for citations of other examples from the literature.

[10] R. Knorr, T. Menke, C. Behringer, K. Ferchland, J. Mehlstäubl, E. Lattke, Organometallics 32, 2013, 4070–4081.

[11] R. Knorr, E. Lattke, E. Räpple, Liebigs Ann. Chem. 1980, 1207–1215, compound **3** therein.

[12] R. Knorr, T. von Roman, J. Freudenreich, T. P. Hoang, J. Mehlstäubl, P. Böhrer, D. S. Stephenson, H. Huber, B. Schubert, Magn. Reson. Chem. 31, 1993, 557–565.

[13] See the Supplementary Material.

[14] Except for the bp of **5**, characterizing properties were not published by: G. B. Reddy, T. Hanamoto, T. Hiyama, Tetrahedron Lett. 32, 1991, 521–524.

[15] R. Knorr, C. Pires, J. Freudenreich, J. Org. Chem. 72, 2007, 6084–6090, refs 20–22 therein, with our protocol on p S5 of that Supporting Information.

[16] R. Knorr, K. Polborn, J. Chem. Soc., Perkin Trans. 2 1991, 1505–1508.

[17] See Scheme 1 in ref [10].

[18] G. Binsch, E. Eliel, H. Kessler, Angew. Chem. 83, 1971, 618–619; Angew. Chem., Int. Ed. 10, 1971, 570–572.

[19] G. Binsch, Top. Stereochem. 3, 1968, 97–192, on p 178 therein.

[20] R. Knorr, T. Menke, K.-O. Hennig, J. Freudenreich, P. Böhrer, B. Schubert, Tetrahedron 2014, 70, 2703–2710.

[21] Compound **24** in ref [20].

[22] Seebach. D.; Neumann, H. Chem. Ber. 1974, 107, 847–853.

[23] Also observed for **6** and in refs [1] and [10] for *p*-substituted 2-(α-trimethylstannyl)-1,1,3,3-tetramethylindanes.

[24] Δδ values of **1b** taken from ref [10], Tables 1 (entry 8) and S8 (entry 7) therein.

[25] Δδ data in ref [1], Table 1 and Chart S2 on p S13 therein.

[26] W. F. Bailey, T. V. Ovaska, J. Am. Chem. Soc. 115, 1993, 3080–3090, Table II therein.

[27] Prepared as reported on p S19 in the Supporting Information of ref [1].

The two new alkenyllithium monomers are microsolvated by 3 THF ligands at Li.

Their rapid stereoinversion is catalyzed by THF via a solvent-separated ion pair.

$Li^{+}(THF)_4$ migrates within the ion pair during sp^2-stereoinversion of the carbanion.

Supplementary Material for

Microsolvation, aggregation, and pseudomonomolecular, ionic sp^2-stereoinversion mechanism of two exocyclic β,β-di-*tert*-alkyl-α-arylvinyllithiums

Rudolf Knorr*, Karsten-Olaf Hennig, Petra Böhrer, Bernhard Schubert

Address: Department Chemie, Ludwig-Maximilians-Universität München, Butenandtstrasse 5-13 (Haus F), 81377 München, Germany

Email: Rudolf Knorr* - rhk@cup.uni-muenchen.de

Contents:

1. Products **8**, **9b**, **9c**, **15c**, and **15d**

*1.1. 3,3,6,6-Tetramethyl-2-phenylcyclohexanone (**8**)*

The crude monobromide **4** was kept at r.t. for seven days and deposited colorless needles **8**: Mp 78–79 °C (pentane); IR (KBr) ν 1705 cm^{-1}; ^{1}H NMR ($CDCl_3$, 400 MHz) δ 0.82 (s, 3H, 1 × 6-CH_3), 0.89 (s, 3H, 1 × 3-CH_3), 1.11 (s, 3H, 1 × 6-CH_3), 1.28 (s, 3H, 1 × 3-CH_3), 1.54 (ddd, 1H, $|^2J|$ 13.6 Hz, ^3J 4.1 Hz, ^3J 2.9 Hz, equat. 4-H), 1.73 (ddd, 1H, $|^2J|$ 13.6 Hz, ^3J 4.1 Hz, ^3J 2.9 Hz, equat. 5-H), 1.89 (broadened td, 1H, $|^2J|$ 13.6 Hz, ^3J 4.2 Hz, ax. 5-H), 2.07 (broadened td, 1H, $|^2J|$ 13.6 Hz, ^3J 4.2 Hz, ax. 4-H), 3.74 (s, 1H, 2-H), 7.18 (dm, 2H, ^3J 7.2 Hz, 2 × *o*-H), 7.24 (tm, 1H, ^3J 7.2 Hz, *p*-H), 7.29 (tm, 2H, ^3J 7.2 Hz, 2 × *m*-H) ppm, assigned through comparison with **7**; ^{13}C NMR ($CDCl_3$, 100.6 MHz) δ 21.72 (1 × 3-CH_3), 25.94 and 26.09 (2 × 6-CH_3), 30.82 (1 × 3-CH_3), 36.62 and 37.44 (CH_2-4/-5), 41.16 (quart., C-3), 44.43 (quart., C-6), 62.90 (*C*H-2), 126.67 (C-*p*), 127.27 (2 × C-*m*), 131.48 (2 × C-*o*), 135.13 (C-*ipso*), 213.42 (C-1) ppm, assigned through comparison with *t*Bu–C(=O)–iPr.

*1.2. α-Phenyl-α-(1,1,3,3-tetramethylcyclopent-2-ylidene)acetic acid (**9b**)*

The bromoalkene **5** (50 mg, 0.17 mmol) and anhydrous *t*BuOMe (0.50 mL) were placed in a dry NMR tube (5 mm) and cooled to –20 °C under argon cover gas. After the introduction of *n*BuLi (0.26 mmol) in hexanes (0.10 mL), the tube was stoppered and kept at 20 °C for two hours. The mixture was poured onto solid CO_2, warmed up, and dissolved in Et_2O together with NaOH (2 M). The acidified alkaline layer furnished the crude acid **9b** (21 mg, < 47%). Mp 171–173 °C (pentane); ^{1}H NMR ($CDCl_3$, 400 MHz) δ 0.87 (s, 6H, 2 × 1-CH_3 cis to phenyl), 1.32 (s, 6H, 2 × 3-CH_3 trans to phenyl), 1.52 (pseudo-t, 2H, CH_2-5), 1.60 (pseudo-t, 2H, CH_2-4), 7.29 (pseudo-s, 5H, phenyl) ppm, assigned through SCS [S1] and comparison with olefin **9a**; ^{13}C NMR ($CDCl_3$, 100.6 MHz) δ 28.12 (2 × 3-CH_3 trans to phenyl), 29.44 (2 × 1-CH_3 cis to phenyl), 40.76 (CH_2-5), 41.04 (CH_2-4), 45.21 (C-3), 45.58 (C-1), 127.47 (C-*p*), 127.60 (2 × C-*m*), 127.76 (C-α), 130.82 (2 × C-*o*), 136.80 (C-*ipso*), 161.57 (C-2), 174.00 (CO_2H) ppm, assigned through comparisons with olefin **15a** and compound **10** in ref [S2].

*1.3. 2-(α-Butylbenzylidene)-1,1,3,3-tetramethylcyclopentane (**9c**)*

This was obtained as a crude liquid from the bromoalkene **5** with *n*BuLi in THF as the solvent. ^{1}H NMR (CCl_4, 80 MHz) δ 0.71 (s, 6H, 2 × 1-CH_3 cis to phenyl), 1.32 (s, 6H, 2 × 3-

CH_3 trans to phenyl), 2.27 (broadened t, 2H, apparent *J* ca. 7.5 Hz, CH_2-1 of butyl), 6.90–7.15 (m, phenyl) ppm, assigned through SCS [S1].

*1.4. 2-(α-Butyl-o,o´-dimethylbenzylidene)-1,1,3,3-tetramethylcyclopentane (**15c**)*

The neutral fractions of several runs with the chloroalkene **13** and *n*BuLi were combined and distilled at 120–150 °C (bath temp.)/0.006 mbar to yield an oil that was enriched with **15c**. ^{1}H NMR ($CDCl_3$, 400 MHz) δ 0.70 (s, 6H, 2 × 1-CH_3 cis to aryl), 0.83 (t, 3H, CH_3 of butyl), ca. 1.20 (overlaid m, CH_2-2/-3 of butyl), 1.37 (s, 6H, 2 × 3-CH_3 trans to aryl), 1.44 (t, 2H, CH_2-5), 1.57 (t, 2H, CH_2-4), 2.22 (s, 6H, 2 × *o*-CH_3), 2.32 (quasi-t, 2H, CH_2-1 of butyl), 6.97 (d, 2H, ^3J 7.3 Hz, 2 × *m*-H), 7.03 (dd, 1H, *p*-H) ppm, assigned through comparison with the olefin **15a**; ^{13}C NMR ($CDCl_3$, 100.6 MHz) δ 14.02 (CH_3 of butyl), 21.31 (2 × *o*-CH_3), 23.64 (CH_2-3 of butyl), 27.57 (2 × 1-CH_3 cis to aryl), 29.30 (2 × 3-CH_3 trans to aryl), 30.33 (CH_2-2 of butyl), 36.14 (CH_2-1 of butyl), 41.91 and 41.99 (CH_2-4/-5), 44.73 and 44.87 (C-1/-3), 125.72 (C-*p*), 127.02 (2 × C-*m*), 132.08 (C-α), 136.08 (2 × C-*o*), 142.26 (C-*ipso*), 151.02 (C-2) ppm, assigned as above.

*1.5. α-(o,o´-Dimethylphenyl)-α-(1,1,3,3-tetramethylcyclopent-2-ylidene)acetic acid (**15d**)*

Colorless crystals; mp 151–152.5 °C (pentane at –20 °C); ^{1}H NMR ($CDCl_3$, 400 MHz) δ 0.85 (s, 6H, 2 × 1-CH_3 cis to aryl), 1.37 (s, 6H, 2 × 3-CH_3 trans to aryl), 1.54 (pseudo-t, 2H, CH_2-5), 1.59 (pseudo-t, 2H, CH_2-4), 2.32 (s, 6H, 2 × *o*-CH_3), 7.00 (d, 2H, ^3J 7.5 Hz, 2 × *m*-H), 7.19 (t, 1H, ^3J 7.5 Hz, *p*-H) ppm, assigned through comparison with the acid **9b**; ^{13}C NMR ($CDCl_3$, 100.6 MHz) δ 21.15 (2 × *o*-CH_3), 27.53 and 27.81 (2 × 1-/3-CH_3), 40.80 (CH_2-5), 41.43 (CH_2-4), 45.45 and 45.88 (C-3/-1), 125.53 (C-α), 127.25 (2 × C-*m*), 127.49 (C-*p*), 135.50 (C-*ipso*), 138.22 (2 × C-*o*), 161.63 (C-2), 174.05 (CO_2H) ppm, assigned as above; IR (KBr) ν 3600–2400 (CO_2H), 1682 (s), 1460, 1266, 1244, 772 cm^{-1}.

1.6. References of Section 1

[S1] R. Knorr, T. von Roman, J. Freudenreich, T. P. Hoang, J. Mehlstäubl, P. Böhrer, D. S. Stephenson, H. Huber, B. Schubert, Magn. Reson. Chem. 1993, 31, 557–565.

[S2] R. Knorr, T. Menke, C. Behringer, K. Ferchland, J. Mehlstäubl, E. Lattke, Organometallics 32, 2013, 4070–4081.

2. Cis/trans sp^2-stereoinversion rate constants

Table S1. Temperature-dependent pseudo-first-order rate constants k_ψ (s^{-1}) of **2a** in THF (see the diagram in Figure 8 of the Main Text)

°C [a]	conc.	1000/*T*	k_ψ	Δk_ψ	ln k_ψ	Δln k_ψ
–36	0.13 M	4.217	18	± 3	2.89	± 0.17
–22	0.06 M	3.982	38	± 3	3.64	± 0.08
–14	0.13 M	3.859	71	± 5	4.26	± 0.07
–5	0.06 M	3.729	112	± 7	4.72	± 0.06
3	0.13 M	3.621	169	± 8	5.13	± 0.05
8	0.05 M	3.557	205	± 10	5.32	± 0.05
15	0.12 M	3.470	275	± 15	5.62	± 0.06

[a] Uncertainty ±0.5 °C.

Table S2. Temperature-dependent pseudo-first-order rate constants k_ψ (s^{-1}) of **2b** in THF

°C [a]	conc.	1000/*T*	k_ψ	Δk_ψ	ln k_ψ	Δln k_ψ
–60	0.20 M	4.619	8	± 3	2.08	± 0.40
–45	0.21 M	4.383	27	± 3	3.30	± 0.11
–33	0.21 M	4.164	59	± 3	4.08	± 0.05
–19	0.21 M	3.935	140	± 20	4.94	± 0.14

[a] Uncertainty ±0.5 °C.

3. Alternative preparation of the α-bromoalkene **5** from olefin **9a**

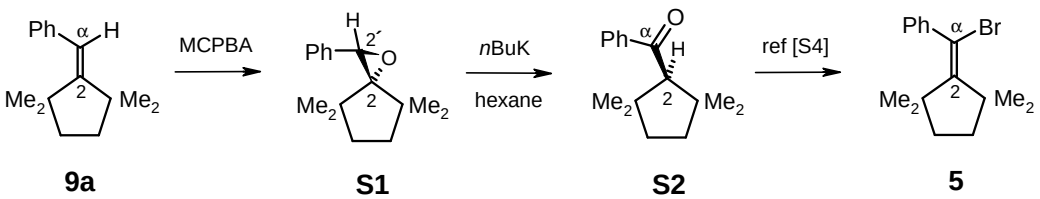

9a **S1** **S2** **5**

Scheme S1. The epoxide **S1** is generated with 3-chloroperbenzoic acid (MCPBA) and isomerized with *n*-butylpotassium.

*3.1. 1,1,3,3-Tetramethylspiro[2´-phenyloxirane-3´,2-cyclopentane (**S1**)]*

A suspension of the olefin **9a** (8.24 g, 38.4 mmol) and $NaHCO_3$ (10.47 g, 125 mmol) in dry chloroform (75 mL) was cooled in an ice bath and stirred during the batchwise addition of 3-chloroperbenzoic acid (85% MCPBA, 10.14 g, 50 mmol). The suspension was stirred for three more hours at r.t., then treated with aqueous NaOH (2 M, 25 mL), and shaken with Et_2O (3 × 50 mL). The combined Et_2O extracts were washed with distilled water until neutral, dried over Na_2SO_4, filtered, and concentrated to yield crude **S1** as an almost pure, solidifying mass (8.22 g, 93%). This material was filtered in petroleum ether as the solvent through Al_2O_3 (basic, Woelm activity I, 1.0 g) that retained a contaminating trace of 3-chlorobenzoyl peroxide. The colorless needles of pure **S1** (7.52 g, 85%) had mp 45.5–47.5 °C (cyclohexane, or low-boiling petroleum ether). ^{1}H NMR (CCl_4, 80 MHz) δ 0.55, 0.83, 0.88, and 1.15 (4 s, 4 × 3H, 2 × 1-/3-CH_3), 1.57 (s, 4H, CH_2-4/-5), 3.74 (s, 1H, 2´-H), 7.20 (quasi-s, 5H, phenyl) ppm; ^{13}C NMR ($CDCl_3$, 20.15 MHz) δ 24.05, 26.62, 27.11, and 27.59 (4 q, 2 × 1-/3-CH_3), 37.50 and 40.53 (2 t, CH_2-4/-5), 40.59 and 42.22 (2 quart., C-1/-3), 59.94 (d, C-2´), 79.27 (quart., C-2), 126.40 and 127.79 (2 d, 2 × C-*o* and 2 × C-*m*), 126.88 (d, C-*p*), 137.09 (quart., C-*ipso*) ppm, assigned through off-resonance {^{1}H} decoupling; IR (KBr) ν 3061 (w), 2962, 2940, 2871, 1497, 1464, 1384, 1369, 1137, 958, 870, 742 (s), 699 (s), 634, 623 cm^{-1}. Anal. calcd for $C_{16}H_{22}O$ (230.35): C, 83.43; H, 9.63. Found: C, 83.13; H, 9.44.

*3.2. 2-Benzoyl-1,1,3,3-tetramethylcyclopentane (**S2**)*

A mixture of dry pentane (50 mL) and *n*BuLi (19.1 mmol) in hexane (7.38 mL) was stirred under argon gas cover in an ice-bath during the batchwise addition of dry potassium *tert*-butoxide (2.14 g, 19.1 mmol). The yellow suspension was stirred at r.t. for 15 min more, cooled again in an ice-bath, treated with the oxirane **S1** (2.00 g, 8.68 mmol), stirred at r.t. for one hour, cooled once more in ice, quenched by the dropwise addition of distilled water, and shaken with Et_2O (3 × 50 mL). The combined Et_2O extracts were washed with distilled water until neutral, dried over Na_2SO_4, and evaporated to yield crude **S2** (1.98 g, 99%) as a solidifying yellow liquid. The colorless needles of pure **S2** had a mp of 30–30.5 °C (low-boiling petroleum ether at 4 °C; ref [S3]: no mp). ^{1}H NMR (CCl_4, 80 MHz) δ 1.05 and 1.12 (2 s, 2 × 6H, 2 × 1-/3-CH_3), 1.63 (m, 4H, CH_2-4/-5), 3.37 (s, 1H, 2-H), 7.30 (m, 3H, 2 × *m*-H and *p*-H), 7.73 (m, 2H, 2 × *o*-H) ppm; ^{13}C NMR ($CDCl_3$, 20.15 MHz) δ 26.47 and 32.05 (2 q, 2 × 1-/3-CH_3), 41.46 (t, CH_2-4/-5), 44.28 (2 × quart., C-1/-3), 64.27 (d, C-2), 127.94 and 128.40 (2 d, 2 × C-*o* and 2 × C-*m*), 132.21 (d, C-*p*), 140.97 (quart., C-*ipso*), 202.69 (C=O)

ppm, assigned through off-resonance {^{1}H} decoupling; IR (KBr) ν 2951 (s), 2869, 1676 (s), 1447, 1368, 1204, 691 cm^{-1}. Anal. calcd for $C_{16}H_{22}O$ (230.35): C, 83.43; H, 9.63. Found: C, 83.55; H, 9.55.

*3.3. 2-(α-Bromobenzylidene)-1,1,3,3-tetramethylcyclopentane (**5**) from **S2***

Pure **5** was obtained through the very slow reaction of 2-benzoyl-1,1,3,3-tetramethylcyclopentane (**S2**) with a large excess of 2,2,2-tribromo-2,2-dihydro-1,3,2-benzodioxaphosphole [S4] in 1,2-dichloroethane at 100 °C within 45 hours.

3.4. References of Section 3

[S3] G. B. Reddy, T. Hanamoto, T. Hiyama, Tetrahedron Lett. 32, 1991, 521–524.

[S4] U. von Roman, J. Ruhdorfer, R. Knorr, Synthesis 1993, 985–992, method A1 therein and quoted literature.

4. X-ray diffraction analysis of dimeric **2a**&1THF

4.1. Crystallographic data, structure solution, and refinement

Formula $C_{20}H_{29}LiO$, weight 292.37; crystal size, 0.4 × 0.3 × 0.3 mm, "colorless square"; crystal system, triclinic, space group P-1; unit cell dimensions, a = 9.742(7) Å, b = 9.847(4) Å, c = 10.999(6) Å, α = 114.57(2)°, β = 93.33(2)°, γ = 107.57(2)°; volume, 894.2(9) Å^3; Z = 2; calculated density, 1.086 Mg/m^3; absorption coefficient, 0.063 mm^{-1}; F(000), 320; diffractometer used, Siemens SMART Area-detector; radiation and wavelength, MoKα with λ = 0.71073 Å; scan type, hemisphere; temperature, 173(3) K; 2θ range for data collection, 4.16 to 58.06°; index ranges, $-12 \le h \le 12$, $-7 \le k \le 13$, $-14 \le l \le 14$; reflections collected, 5323; independent reflections, 2852 (R_{int} = 0.0167); observed reflections, 2327 ($F > 4\sigma(F)$).

1200 frames measured in phi (0–360) with chi=0 and om=2th=25; 65 frames measured in om (15–35) with chi=280, 2th=29 and phi=0; crystal mounted in perfluoropolyether oil.

Structure solution programm, SHELXS (Sheldrick 1997); solution, direct methods; refinement method, full-matrix least-squares on F^2; hydrogen atoms, mixed; weighting scheme, $w^{-1} = \sigma^2Fo^2 + (0.05040P)^2 + 0.5352P$ where $P = (Fo^2 + 2\,Fc^2)/3$; data/restraints/parameters, 2852 / 0 / 203; data-to-parameter ratio, 14.0:1 (11.5:1 [$F > 4\sigma(F)$]); final R indices [$F > 4\sigma(F)$], R1 = 0.0515, wR2 = 0.1249; R indices (all data), R1 = 0.0637, wR2 = 0.1340; goodness-of-fit on F^2, 1.030; largest and mean Δ/σ, 0.000 0.000; largest difference peak, 0.323 eÅ^{-3}; largest difference hole, –0.313 eÅ^{-3}; refinement program used, SHELXL (Sheldrick 1997); CifRtf version used, 2.0.

4.2. Selected topologic parameters

Table S3. Selected interatomic distances (Å), angles (°), and dihedral angles (°) of the crystalline, disolvated dimer (**2a**&1THF)$_2$ at –100 °C. [a]

parameter	value	parameter	value	parameter	value
O1-C10	1.428(3)	O1-C13	1.436(3)	O1-Li1	1.943(3)
Li1-C14	2.204(4)	Li1-C14A	2.203(4)	Li1-Li1A	2.456(7)
Li1-C15	2.661(4)	C1-C2	1.556(3)	C1-C5	1.533(3)
C1-C6	1.529(3)	C1-C7	1.528(3)	C1-C15	3.138
C2-C3	1.547(3)	C2-C14	1.343(3)	C3-C4	1.537(3)
C3-C8	1.534(3)	C3-C9	1.522(2)	C4-C5	1.526(3)
C6-C15	3.447	C6-C16	3.685	C7-C15	3.247
C7-C20	3.334	C10-C11	1.461(3)	C11-C12	1.477(4)
C12-C13	1.500(3)	C14-Li1A	2.203(4)	C14-C15	1.475(3)
C15-C16	1.410(3)	C15-C20	1.407(3)	C16-C17	1.375(3)
C17-C18	1.383(3)	C18-C19	1.388(3)	C19-C20	1.380(2)
C10-O1-C13	106.98(16)	C10-O1-Li1	123.03(18)	C13-O1-Li1	127.87(16)
O1-Li1-C14	121.67(16)	O1-Li1-C14A	122.80(17)	O1-Li1-Li1A	163.2(3)
O1-Li1-C15	117.24(15)	C14-Li1-C14A	112.27(15)	C14-Li1-C15	33.67(8)
C14-Li1-Li1A	56.11(14)	C14A-Li1-Li1A	56.15(13)	C14A-Li1-C15	117.93(14)
C15-Li1-Li1A	70.93(15)	C2-C1-C5	104.18(16)	C2-C1-C6	109.43(16)
C2-C1-C7	114.58(17)	C5-C1-C6	109.15(19)	C5-C1-C7	109.43(17)
C6-C1-C7	109.84(19)	C1-C2-C3	107.67(16)	C1-C2-C14	128.74(17)
C3-C2-C14	123.56(16)	C2-C3-C4	103.87(16)	C2-C3-C8	109.85(16)
C2-C3-C9	114.02(16)	C4-C3-C8	110.47(18)	C4-C3-C9	111.18(17)
C8-C3-C9	107.47(16)	C3-C4-C5	103.82(18)	C1-C5-C4	104.82(17)
O1-C10-C11	109.1(2)	C10-C11-C12	106.3(2)	C11-C12-C13	104.9(2)
O1-C13-C12	105.93(18)	Li1-C14-Li1A	67.73(15)	C2-C14-Li1	137.06(16)
C2-C14-Li1A	117.60(17)	C2-C14-C15	123.80(16)	C15-C14-Li1	90.40(16)
C15-C14-Li1A	106.18(15)	C14-C15-Li1	55.94(13)	C14-C15-C16	122.06(17)
C14-C15-C20	122.17(16)	C16-C15-Li1	119.67(14)	C16-C15-C20	115.05(18)
C20-C15-Li1	89.12(13)	C15-C16-C17	122.48(19)	C16-C17-C18	121.0(2)
C17-C18-C19	118.3(2)	C15-C19-C20	122.55(18)	C18-C19-C20	120.6(2)
C1-C2-C14-Li1	–140.42	C1-C2-C14-C15	3.4	C2-C1-C5-C4	29.60
C2-C3-C4-C5	34.42	C2-C14-C15-C16	101.32	C2-C14-C15-C20	88.88
C3-C4-C5-C1	40.40				

[a] Symmetry operations used for equivalent atoms ("A"): –x+1; –y+1; –z.

Table S4. Atomic coordinates ($\times 10^4$) and equivalent isotropic displacement parameters ($Å^2 \times 10^3$) for the crystalline dimer (**2a**&1THF)$_2$. U(eq) is defined as one third of the trace of the orthogonalized *Uij* tensor. [a]

atom	x	y	z	U(eq)
O1	3707.3(15)	7319.2(18)	2109.5(13)	36.1(4)
Li1	4650(4)	6094(4)	788(3)	35.9(8)
C1	7883.2(19)	4893(2)	3159.4(18)	29.0(5)
C2	6513.0(18)	4547(2)	2123.1(16)	23.6(4)
C3	5287(2)	3031(2)	1986.5(17)	27.0(4)
C4	6110(2)	2274(3)	2596(2)	41.2(5)
C5	7326(2)	3710(3)	3745(2)	38.5(5)
C6	9086(2)	4513(3)	2394(2)	49.3(7)
C7	8506(2)	6598(3)	4326(2)	43.9(6)
C8	4154(2)	3507(3)	2822(2)	41.7(6)
C9	4456(2)	1862(2)	523.3(18)	32.6(5)
C10	3624(3)	7297(4)	3394(2)	63.0(8)
C11	2884(3)	8373(4)	4151(2)	57.7(7)
C12	2493(3)	9044(4)	3263(2)	57.3(7)
C13	2667(3)	7997(3)	1875(2)	43.6(6)
C14	6364.2(19)	5337(2)	1410.0(16)	25.3(4)
C15	7520.1(19)	6797(2)	1552.5(17)	24.8(4)
C16	8431(2)	6764(3)	597.4(19)	31.2(5)
C17	9369(2)	8134(3)	613(2)	38.3(5)
C18	9461(2)	9628(3)	1580(2)	40.1(5)
C19	8578(2)	9712(3)	2535(2)	38.1(5)
C20	7636(2)	8336(2)	2517.5(18)	30.5(5)

[a] Symmetry operations used for equivalent atoms ("A"): –x+1; –y+1; –z.

Table S5. Anisotropic displacement parameters ($Å^2 \times 10^3$) for the dimer (**2a**&1THF)$_2$.

atom	U11	U22	U33	U23	U13	U12
O1	43.6(8)	45.5(10)	30.4(7)	17.6(6)	13.6(6)	29.2(7)
Li1	42.0(18)	41(2)	24.6(15)	9.4(14)	5.5(13)	22.7(16)
C1	30.9(9)	30.0(12)	27.4(9)	14.9(8)	2.5(7)	10.8(8)
C2	28.6(8)	23.6(10)	19.1(7)	8.0(7)	5.8(6)	12.3(8)
C3	34.1(9)	23.8(11)	24.7(8)	12.2(8)	4.6(7)	11.0(8)
C4	48.7(12)	34.0(12)	42.6(11)	23.5(10)	–2.5(9)	10.6(10)
C5	44.5(11)	38.4(13)	36.2(10)	23.1(10)	–1.0(8)	12.7(10)
C6	39.8(11)	76(2)	50.4(13)	36.6(13)	12.0(9)	32.1(12)
C7	49.6(12)	37.2(13)	34.7(10)	15.3(10)	–10.2(9)	7.2(11)
C8	42.1(11)	40.0(14)	38.5(11)	15.4(11)	16.8(9)	10.8(10)
C9	36.3(10)	25.6(11)	30.4(9)	10.6(8)	2.2(7)	7.8(9)
C10	99(2)	88(2)	37.5(12)	34.9(14)	29.9(13)	69.1(19)
C11	78.5(17)	71(2)	43.2(13)	28.4(13)	26.8(12)	46.7(16)
C12	86.2(18)	66.2(19)	52.5(14)	33.7(14)	36.0(13)	57.2(16)
C13	52.1(12)	57.0(16)	40.6(11)	26.7(11)	17.0(9)	36.7(12)
C14	29.0(9)	26.4(11)	21.0(8)	9.7(8)	5.6(6)	12.0(8)
C15	28.2(8)	27.3(11)	23.8(8)	14.2(8)	3.1(6)	13.0(8)
C16	37.9(10)	32.3(12)	31.5(9)	17.3(9)	11.0(8)	18.5(9)
C17	37.5(10)	48.7(15)	45.8(11)	32.3(11)	16.9(9)	20.8(11)
C18	37.9(11)	34.9(13)	54.3(13)	29.8(11)	8.1(9)	8.5(10)
C19	43.7(11)	26.9(12)	41.7(11)	14.2(9)	4.8(9)	13.0(10)
C20	36.5(10)	27.5(12)	28.8(9)	13.2(8)	8.0(7)	12.4(9)

Table S6. Hydrogen coordinates ($\times 10^4$) and equivalent isotropic displacement parameters ($Å^2 \times 10^3$) for the dimer (**2a**&1THF)$_2$.

atom	x	y	z	U(eq)
H(4A)	5459	1636	2951	49
H(4B)	6522	1603	1916	49
H(5A)	8112	3398	3991	46
H(5B)	6940	4179	4550	46
H(6A)	8709	3418	1705	59
H(6B)	9915	4681	3027	59
H(6C)	9389	5201	1971	59
H(7A)	7721	6879	4727	53
H(7B)	8973	7325	3976	53
H(7C)	9216	6659	5008	53
H(8A)	4650	4270	3748	50
H(8B)	3457	2574	2815	50
H(8C)	3648	3974	2428	50
H(9A)	3915	2345	182	39
H(9B)	3784	908	505	39
H(9C)	5143	1594	–40	39
H(10A)	4607	7638	3915	76
H(10B)	3079	6219	3245	76
H(11A)	3534	9221	5006	69
H(11B)	2005	7792	4353	69
H(12A)	3147	10143	3586	69
H(12B)	1486	9013	3239	69
H(13A)	1731	7160	1333	52
H(13B)	3031	8621	1396	52
H(16A)	8395	5778	–68	37
H(17A)	9951	8054	–37	46
H(18A)	10098	10553	1590	48
H(19A)	8621	10705	3193	46
H(20A)	7056	8429	3169	37

5. Tabulated primary NMR data

Table S7. Temperature dependence of the ^{1}H NMR chemical shifts δ_H [ppm] of the α-phenyl compound **2a** in THF at 400 MHz, with coupling constants [Hz] in parentheses [a]

temp.	conc.	chemical shifts δ [ppm]					
°C	[**2a**]	*m*-H	*o*-H	*p*-H	one CH_2	3-CH_3	1-CH_3
+55	0.005	6.747 (t)	6.463 (d)	6.195 (t)	–	1.056	
+40	0.031	6.742 (t 7.5)	6.461 (dd 8.0, 1.2)	6.190 (tt 7.0, 1.3)	–	1.054	
+25	0.057	6.74 (t 7.5)	6.47 (d 8.0)	6.18 (t 7.0)	–	1.053	
+15	0.121	6.73 (t 7.5)	6.454 (d 8.0)	6.176 (tt 7.0, 1.3)	–	1.050	
+8	0.045	6.73 (t 7.5)	6.46 (d 8.0)	6.18 (t 7.0)	–	1.052	
+3	0.132	6.724 (t 7.5)	6.45 (d 8.0)	6.17 (tt 7.0, 1.3)	–	1.050	
–5	0.064	6.73 (t 7.5)	6.45 (d 8.0)	6.174 (t 7.0)	–	1.053	
–14	0.127	6.72	6.45 (d)	6.17	1.41 vbr	1.050	
–22	0.062	6.73 (t 7.5)	6.45 (dd 8.0)	6.17 (tt 7.0, 1.3)	1.41 br	1.053 vbr	
–36	0.130	6.722 (t 7.5)	6.442 (d 8.0)	6.167 (tt 7.0, 1.3)	1.395 (brd t)	1.074	1.026
–50	0.058	6.73 (t 7.5)	6.45 (d 8.0)	6.17 (t 7.0)	1.395	1.075	1.029
–66	0.127	6.725 (t 7.5)	6.440 (d 8.0)	6.165 (t 7.0)	1.392 (t)	1.074	1.028
–82	0.139	6.73 (t 7.5)	6.44 (d 8.0)	6.166 (t 7.0)	1.392 (t)	1.074	1.030
Δδ [b]	–	–0.53	–0.71	–0.99	–	–0.10	+0.05

(a) br = broad, brd = broadened, vbr = very broad. (b) Δδ = δ(RLi) – δ(RH) at –82 °C.

Table S8. Temperature dependence of the ^{1}H NMR chemical shifts δ_H [ppm] of the 2,6-dimethylphenyl compound **2b** in THF at 400 MHz, with coupling constants [Hz] in parentheses [a]

temp.	conc.	chemical shifts δ [ppm]				
°C	[**2b**]	*m*-H	*p*-H	*o*-CH_3	3-CH_3	1-CH_3
+25	0.084	6.59 (d 7.2)	6.22 (t 7.2)	2.06	1.035	
+10	0.183	6.57 (d 7.2)	6.205 (t 7.2)	2.06	1.03	
–4	0.189	6.57 (d 7.2)	6.20 (t 7.2)	2.063	1.038 vbr	
–19	0.214	6.57 (d 7.2)	6.20 (t 7.2)	2.06	(1.12) vbr	
–33	0.206	6.57 (d 7.2)	6.20 (t 7.2)	2.063	1.146	–
–45	0.210	6.57 (d 7.2)	6.20 (t 7.2)	2.06	1.150	0.92
–60	0.201	6.57 (d 7.2)	6.20 (t 7.2)	2.06	1.145	0.924
–85	0.192	6.58 (d 7.0)	6.20 (t 7.0)	2.06	1.14	0.93
Δδ [b]	–	–0.40	–0.83	–0.14	–0.09	+0.02

(a) vbr = very broad. (b) Δδ = δ(RLi) – δ(RH) at –85 °C.

Table S9. Temperature dependence of the ^{1}H NMR chemical shifts δ_H [ppm] of the α-phenyl compound **2a** in [D_8]toluene with THF at 400 MHz, with coupling constants [Hz] in parentheses [a]

temp.	conc.	conc.	Agg. [b]	chemical shifts δ [ppm]						
°C	[**2a**]	[THF]	(%)	*m*-H	*p*-H	*o*-H	4-H	5-H	1-CH_3	3-CH_3
+25	0.12	0.26	D (+ M)	7.14 (t 7.5)	6.75 (t 7.3)	6.67 (d 7.5)	1.63	1.60	1.26	0.85 brd
+3	0.12	0.28	D (+ M)	7.16 (t 7.5)	6.77 (t 7.4)	6.68 (d 7.5)	1.64 vbr	1.61 vbr	1.28	0.83 br
–15	0.11	0.28	D (+ M)	7.19 (t 7.5)	6.80 (t 7.2)	6.69 (d 7.5)	1.65 brd	1.62 brd	1.293	0.83 brd
–32	0.11	0.30	D (+ M)	7.22 (t 7.5)	6.82 (t 7.2)	6.70 (d 7.5)	1.66 brd	1.63 brd	1.316	0.83 brd
–45	0.12	0.29	D	7.24 (t 7.5)	6.84 (t 7.3)	6.72 (d 7.5)	1.67	1.64	1.338	0.834
			M (5.3 ± 0.6)	–	6.64 (t)	ca. 6.86	2.01 vbr	1.88 vbr	–	(1.6) vbr
–58	0.11	0.28	D	7.265 (t 7.5)	6.860 (t 7.4)	6.727 (d 7.5)	1.68 br	1.66 br	1.36	0.840
			M (11 ± 3)	7.197 (t 8)	6.68 (t 7)	ca. 6.87	–	1.90	1.40	1.61
–70	0.12	0.28	D	7.291 (t 7.5)	6.879 (t 7.4)	6.741 (d 7.5)	1.697 br	1.68 br	1.38	0.85
			M (15 ± 3)	7.213 (t 7.5)	6.692 (t 7.4)	6.902 (d)	2.08 (t)	1.93 (t)	1.43	1.65
–83	0.11	0.28	D	7.312 (t 7.5)	6.894 (t 7.4)	6.752 (d 7.5)	1.70 br	1.68 br	1.395	0.867
			M (18 ± 2)	7.23 (t 7.5)	6.71 (t 7.4)	ca. 6.92 (d)	2.11 (t)	1.96 (t)	–	1.70
–96	0.12	0.29	D	7.349 (t 7.3)	ca. 6.92	6.778 (d 7.5)	(1.73) vbr	(1.73) vbr	–	0.87 vbr
			M (28 ± 2)	7.262 (t 7.5)	6.74 (t 7.4)	6.964 (d 7.7)	2.167 br	2.01 br	–	–
Δδ [c]			D	+0.10	–0.24	–0.37	+0.12	+0.15	+0.35	–0.28
Δδ [c]			M	+0.02	–0.42	ca. –0.2	+0.53	+0.43	–	+0.55

(a) br = broad, brd = broadened, vbr = very broad. (b) Agg.: D = dimer, M = monomer. (c) Δδ = δ(RLi) – δ(RH) at –83 °C.

Table S10. Temperature dependence of the ^{13}C NMR chemical shifts δ_C [ppm] of the α-phenyl compound **2a** in THF at 100.6 MHz [a]

temp.	conc.	chemical shifts δ [ppm]											
°C	[**2a**]	C-α	C-*i*	C-2	C-*m*	C-*o*	C-*p*	C-1	C-3	C-5	C-4	3-CH_3	1-CH_3
+40	0.031	–	162.6	148.6	127.16	121.7	114.06	ca. 45.9 vbr		ca. 41.1 vbr		32.63	
+25	0.057	185.3	162.8	148.3	127.01	121.7	113.9	(46.4) vbr	(44.6) vbr	ca. 41.1 vbr		32.63 br	
+15	0.121	185.6	162.9	148.05	127.0	121.7	113.8	47.0 vbr	44.2 vbr	(42.0)	(40.4)	32.62	
+8	0.045	185.8	163.0	148.0	126.95	121.7	113.74	47.2 br	44.2 br	42.3 br	40.3 br	32.6 vbr	
+3	0.132	185.9	163.05	147.83	126.9	121.7	113.7	47.2 br	44.0 br	42.4 br	40.3 br	32.6 xbr	
–5	0.064	186.0	163.1	147.75	126.9	121.7	113.65	47.2 br	44.1 br	42.4 br	40.3 br	(32.9)	(32.4)
–14	0.127	186.2	163.17	147.55	126.86	121.7	113.6	47.2 brd	44.05 brd	42.4 brd	40.2 brd	32.95	32.2
–22	0.062	186.3	163.2	147.46	126.85	121.7	113.53	47.2 brd	44.0 brd	42.4 brd	40.2 brd	32.96 brd	32.14 brd
–36	0.130	186.5	163.2	147.2	126.82	121.6	113.43	47.2	44.0	42.3	40.15	32.93	32.12
–50	0.058	186.75 br	163.2	147.07	126.82	121.6	113.41	47.2	44.0	42.3	40.13	32.93	32.11
–66	0.127	186.74 [b]	163.2	146.83	126.82	121.5	113.34	47.2	44.0	42.2	40.1	32.90	32.08
–82	0.139	186.86 [c]	163.2	146.63	126.83	121.4	113.29	47.2	44.0	42.2	40.05	32.88	32.07
Δδ [d]	–	+65.1	+23.4	–15.3	–1.5	–8.3	–13.4	+2.3	–0.4	+0.6	+1.5	+1.6	+2.8

(a) br = broad, brd = broadened, vbr = very broad, xbr = extremely broad. (b) brd t $^1J_{C,Li}$ = 10.7 Hz. (c) sharp t $^1J_{C,Li}$ = 10.7 Hz. (d) Δδ = δ(RLi) – δ(RH) at –82 °C.

Table S11. Temperature dependence of the ^{13}C NMR chemical shifts δ_C [ppm] of the 2,6-dimethylphenyl compound **2b** in THF at 100.6 MHz [a]

temp.	conc.	chemical shifts δ [ppm]												
°C	[**2b**]	C-α	C-*i*	C-2	C-*m*	C-*o*	C-*p*	C-1	C-3	C-5	C-4	3-*C*H$_3$	1-*C*H$_3$	*o*-*C*H$_3$
+25	0.084	181.94	158.3	144.4	126.5	125.0	114.93	44.69		41.05 br		ca. 31.1 br		22.2
+10	0.183	182.4	158.7	144.0	126.4	125.05	114.83	44.76		41.15 vbr		ca. 31.1 vbr		22.25
–4	0.189	182.7	158.8	143.7	126.4	125.1	114.74	44.82		41.15 vbr		31.1 vbr		22.33
–19	0.214	182.96	159.0	143.3	126.3	125.1	114.64	44.87 br		(42.0)	(40.3)	32.2	(29.9)	22.40
–33	0.206	183.1	159.1	143.1	126.3	125.1	114.60	44.90 vbr		42.05	40.24	32.17	(29.9)	22.48
–45	0.210	183.2	159.1	142.9	126.3	125.1	114.5	(45.04)	(44.81)	42.05	40.21	32.12	29.97	22.54
–60	0.201	183.23 [b]	159.0	142.5	126.2	125.0	114.4	44.98	44.80	41.98	40.16	32.0	29.93	22.54
–85	0.192	183.26 [c]	158.9	142.1	126.16	124.9	114.26	44.91	44.83	41.90	40.10	31.91	29.98	22.64
Δδ [d]	–	+64.0	+20.8	–17.4	–1.2	–11.5	–12.6	+1.1	–0.6	+0.9	+1.3	+1.4	+2.0	+1.4

(a) br = broad, vbr = very broad. (b) brd t $^1J_{C,Li}$ = ca. 10.2 Hz. (c) sharp t $^1J_{C,Li}$ = 10.7 Hz. (d) Δδ = δ(RLi) – δ(RH) at –85 °C.

Table S12. Temperature dependence of the ^{13}C NMR chemical shifts δ_C [ppm] of the α-phenyl compound **2a** in [D_8]toluene with THF at 100.6 MHz [a]

temp.	conc.	conc.	Agg. [b]	chemical shifts δ [ppm]											
°C	[**2a**]	[THF]	(%)	C-α	C-2	C-*i*	C-*m*	C-*o*	C-*p*	C-1	C-3	C-5	C-4	3-*C*H_3	1-*C*H_3
+25	0.12	0.26	D (+ M)	173.3 br	161.6 br	158.6	128.3	122.7	118.5	47.3	44.4	41.9	39.8	31.68 brd	31.64
+3	0.12	0.28	D (+ M)	173.1 vbr	161.5 brd	158.5	128.3	122.6	118.5	47.2	44.4	41.8	39.8	31.5 brd	31.60
–15	0.11	0.28	D (+ M)	173.1 [c]	161.34	158.4	128.33	122.6	118.5	47.2	44.4	41.7	39.7	31.37	31.55
–32	0.11	0.30	D	173.0 [d]	161.20	158.45	128.4	122.53	118.45	47.20	44.40	41.58	39.62	31.27	31.53
			M (–)	–	–	–	–	121.3	115.0	–	–	–	–	–	32.2
–45	0.12	0.29	D	172.96 [e]	161.10	158.45	128.4	122.50	118.44	47.19	44.40	41.49	39.58	31.18 brd	31.51
			M (5.3 ± 0.6)	–	–	ca. 162.4	–	121.1 vbr	114.5 vbr	–	–	–	–	33.1	32.3
–58	0.11	0.28	D	172.94 [e]	161.00	158.46	128.4	122.46	118.41	47.17	44.41	41.43	39.53	31.11	31.50
			M (11 ± 3)	–	–	162.3 br	–	121.3	114.3	–	44.1 br	42.0	39.8	33.0	32.3
–70	0.12	0.28	D	172.91 [e]	160.93	158.48	128.4	122.44	118.40	47.17	44.42	41.39	39.50	31.04	31.49
			M (15 ± 3)	184.4 br	–	162.5 br	–	121.4	114.1	47.23	44.1	42.0	39.9	33.07	32.34
–83	0.11	0.28	D	172.90 [e]	160.85	158.50	128.4	122.42	118.40	47.14	44.44	41.36	39.46	30.98	31.48
			M (18 ± 2)	185.2 br	147.7	162.9	127.2	121.40	113.9	47.3	44.07	42.04	39.99	33.07	32.37
–96	0.12	0.29	D	172.88 [c]	160.78	158.53	–	122.41	118.40	47.13	44.47	41.30	39.43	30.92	31.47
			M (28 ± 2)	185.6 br	147.4	163.1	127.2	121.38	113.8	47.40	44.07	42.07	40.03	33.11	32.40
Δδ [f]	–	–	D	+51.5	–0.8	+19.0	+0.5	–7.4	–7.8	+2.6	+0.4	+0.2	+1.3	–0.1	+2.2
Δδ [f]	–	–	M	+63.8	–13.9	+23.4	–0.7	–8.4	–12.3	+2.8	+0.1	+0.8	+1.8	+2.0	+3.1

(a) br = broad, brd = broadened, vbr = very broad; CH_3 assigned through two-dimensional HETCOR at 25 °C. (b) Agg.: D = dimer, M = monomer. (c) brd qi $^1J_{C,Li}$ = ca. 7.4 Hz. (d) qi $^1J_{C,Li}$ = 7.5 Hz. (e) sharp qi $^1J_{C,Li}$ = 7.5 Hz. (f) Δδ = δ(RLi) – δ(RH) at –83 °C.